

**Synthesis and Strategies to Improve Electrochemical
Performance of Iron-Carboxylate MOF-based Electrodes
for High-Performance Supercapacitors**



By

Sarah Hakeem

Registration No: 00000328094

Department of Materials Engineering

School of Chemical and Materials Engineering

National University of Sciences & Technology (NUST)

Islamabad, Pakistan

(2024)

**Synthesis and Strategies to Improve Electrochemical
Performance of Iron-Carboxylate MOF-based Electrodes
for High-Performance Supercapacitors**



By

Sarah Hakeem

(Registration No: 00000328094)

A thesis submitted to the National University of Sciences and Technology, Islamabad,

in partial fulfillment of the requirements for the degree of

Master of Science in
Materials and Surface Engineering

Supervisor: Dr. M Talha Masood

Co-Supervisor: Dr. Ghulam Ali

School of Chemical and Materials Engineering

National University of Sciences & Technology (NUST)

Islamabad, Pakistan

(2024)



THESIS ACCEPTANCE CERTIFICATE

Certified that final copy of MS thesis written by Ms Sarah Hakeem (Registration No 00000328094), of School of Chemical & Materials Engineering (SCME) has been vetted by undersigned, found complete in all respects as per NUST Statues/Regulations, is free of plagiarism, errors, and mistakes and is accepted as partial fulfillment for award of MS degree. It is further certified that necessary amendments as pointed out by GEC members of the scholar have also been incorporated in the said thesis.

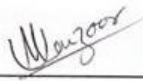
Signature: 

Name of Supervisor: **Dr Muhammad Talha Masood**

Date: 20/09/2024

Signature (HOD): 

Date: 24/9/24

Signature (Dean/Principal): 

Date: 26/9/24

MSE-15-2020



Form TH-1

National University of Sciences & Technology (NUST)

MASTER'S THESIS WORK

Formulation of Guidance and Examination Committee (GEC)

Name: Sarah Hakeem NUST Reg No: 00000328094
 Department: Department of Materials Engineering Specialization: Master of Science in Materials & Surface Engineering
 Credit Hour Completed: 24.0 CGPA: 3.06

Course Work Completed

S/No:	Code:	Title:	Core/Elective:	CH:	Grade:
1.	MSE-881	Manufacturing Processes	Compulsory	3.0	B
2.	MSE-811	Materials Thermodynamics	Compulsory	3.0	B
3.	MSE-812	Phase Transformation & Microstructures	Compulsory	3.0	B
4.	MSE-851	Surface Engineering & Characterisation	Compulsory	3.0	B
5.	ESE-904	Advanced Energy Materials: Synthesis & Characterization	Elective	3.0	B
6.	MSE-821	Mechanical Behaviour Of Materials	Compulsory	3.0	B+
7.	RM-898	Research Methodology	Additional	2.0	Q
8.	NSE-813	Essentials of Nanoscience and Engineering	Elective	3.0	B
9.	MSE-854	Characterization Of Materials	Elective	3.0	B

Date 03 - Nov - 2022

Student's Signature

Thesis Committee

- Name: Zeeshan Ali (Supervisor)
Department: Department of Materials Engineering
Signature:
- Name: Ghulam Ali (Cosupervisor)
Department: Department of Energy Systems Engineering
Signature:
- Name: Muhammad Talha Masood (Internal)
Department: Department of Materials Engineering
Signature:
- Name: Sofia Javed (Internal)
Department: Department of Materials Engineering
Signature:
- Name: Mohsin Saleem (Internal)
Department: Department of Materials Engineering
Signature:

Date: 03 - Nov - 2022

Signature of Head of Department:

APPROVAL



National University of Sciences & Technology (NUST)

FORM TH-4

MASTER'S THESIS WORK

We hereby recommend that the dissertation prepared under our supervision by
Regn No & Name: 00000328094 Sarah Hakeem

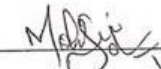
Title: Synthesis and Strategies to Improve Electrochemical Performance of Iron-Carboxylate
MOF-based Electrodes for High Performance Supercapacitors.

Presented on: 05 Sep 2024 at: 1500 hrs in SCME (Seminar Hall)


Be accepted in partial fulfillment of the requirements for the award of Masters of Science
degree in Materials & Surface Engineering.

Guidance & Examination Committee Members

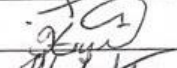
Name: Dr Mohsin Saleem

Signature: 

Name: Dr Sofia Javed

Signature: 

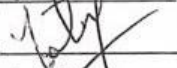
Name: Dr Iftikhar Hussain Gul

Signature: 

Name: Dr Ghulam Ali (Co-Supervisor)

Signature: 

Supervisor's Name: Dr Muhammad Talha Masood


Signature: 

Dated: 18/09/2024



Head of Department

Date 19-09-24



Dean/Principal

Date 19/9/24

School of Chemical & Materials Engineering (SCME)

AUTHOR'S DECLARATION

I **Sarah Hakeem** hereby state that my MS thesis titled “**Synthesis and Strategies to Improve Electrochemical Performance of Iron-Carboxylate MOF-based Electrodes for High-Performance Supercapacitors**” is my own work and has not been submitted previously by me for taking any degree from National University of Sciences and Technology, Islamabad, or anywhere else in the country/ world.

At any time if my statement is found to be incorrect even after I graduate, the university has the right to withdraw my MS degree.

Name of Student: Sarah Hakeem

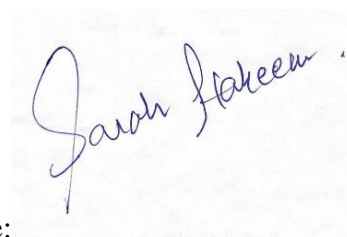
Date: 05/09/24

PLAGIARISM UNDERTAKING

I solemnly declare that the research work presented in the thesis titled “**Synthesis and Strategies to Improve Electrochemical Performance of Iron-Carboxylate MOF-based Electrodes for High-Performance Supercapacitors**” is solely my research work with no significant contribution from any other person. Small contribution/ help wherever taken has been duly acknowledged and that complete thesis has been written by me.

I understand the zero-tolerance policy of the HEC and the National University of Sciences and Technology (NUST), Islamabad towards plagiarism. Therefore, I as an author of the above titled thesis declare that no portion of my thesis has been plagiarized and any material used as reference is properly referred to/cited.

I undertake that if I am found guilty of any formal plagiarism in the above-titled thesis even after award of MS degree, the University reserves the rights to withdraw/revoke my MS degree and that HEC and NUST, Islamabad have the right to publish my name on the HEC/University website on which names of students are placed who submitted plagiarized thesis.

A handwritten signature in blue ink that reads "Sarah Hakeem". The signature is written in a cursive style with a period at the end.

Student Signature:

Name: Sarah Hakeem

DEDICATION

This project is wholeheartedly dedicated to my beloved parents who have been a constant source of inspiration and gave me strength when I thought of giving up. Thank you for bearing with my daily meltdowns and tantrums.

ACKNOWLEDGEMENTS

Alhamdulillah (Praise be to Almighty Allah), I would like to thank Almighty Allah for giving me the opportunity, determination, and strength for this project. His continuous grace and mercy were with me throughout my life and ever more during the tenure of this project.

I would also like to thank and express my deep and sincere gratitude to my very patient and supportive supervisor, **Prof. Dr. M. Talha Masood**, for providing guidance and feedback throughout this project.

Besides my supervisor, I would also like to thank **Prof. Dr. Zeeshan Ali**, for his guidance and constant support.

I would finally like to thank **Mr. Rehan Ullah**, **Miss Ayesha Siddique** for their invaluable help, constructive comments, and suggestions throughout the experimental and thesis work that have contributed to the success of this project.

TABLE OF CONTENTS

DEDICATION	VIII
ACKNOWLEDGEMENTS	IX
TABLE OF CONTENTS	X
LIST OF TABLES	XII
LIST OF FIGURES	XIII
ABSTRACT	XV
CHAPTER 1: INTRODUCTION	1
1.1 Increasing Demand for Energy	1
1.2 Pollution	1
1.3 Climate Change and Renewable Energy	2
1.4 Energy storage devices	4
1.4.1 Batteries	5
1.4.2 Supercapacitors	6
1.5 Objectives	15
CHAPTER 2: LITERATURE REVIEW	17
2.1 MOFs	17
2.1.1 MOFs for next-generation energy storage devices	17
2.1.2 Transition Metal MOFs	17
2.1.3 MOF Linkers	18
2.1.4 MOF Uses	18
2.1.5 MOFs for energy storage	19
2.1.6 Synthetic Approaches for MOFs	20
2.1 Graphene	21
2.3 Methods	23
2.3.1 Hydrothermal/Solvothermal Method	23
2.3.2 Slow Diffusion Method	24
2.3.3 Electrochemical Method	25
2.3.4 Mechanochemical Method	25
2.3.5 Microwave Method	26
2.3.6 Ultrasonic Method	27
CHAPTER 3: EXPERIMENTATION/SYNTHESIS	28
3.1 Materials Required	28
3.2 Apparatus Used	28
3.3 Synthesis of Iron-Carboxylate MOF	29

3.4 Synthesis of Iron-Carboxylate MOF/Graphene	30
3.5 Synthesis of Iron-Copper MOF/Graphene oxide	30
CHAPTER 4: CHARACTERIZATION TECHNIQUES	32
4.1 Scanning Electron Microscopy (SEM) Analysis	32
4.2 X-Ray Diffraction (XRD) Analysis	33
4.3 RAMAN Spectroscopy	34
4.4 Fourier Transform Infrared (FTIR) Spectroscopy	34
4.5 Electrochemical Analysis	35
4.5.1 CV (Cyclic Voltametry)	36
4.5.2 Galvanostatic Charge Discharge (GCD)	37
4.5.3 EIS (Electrochemical Impedance Spectroscopy)	38
CHAPTER 5: RESULTS	40
5.1 XRD Results	40
5.2 SEM results	41
5.3 FTIR Results	43
5.4 Raman Results	45
5.5 Electrochemical Testing	46
5.5.1 CV (Cyclic Voltammetry)	47
5.5.2 GCD (Galvanostatic Charge/Discharge)	48
5.5.3 EIS (Electrochemical Impedance Spectroscopy)	50
5.5.4 Cyclic Stability	51
CHAPTER 6: CONCLUSION	52
Future Outlook	52
REFERENCES	54

LIST OF TABLES

	Page No.
Table 1: Energy Storage Devices	5
Table 2: The pros and cons of Primary and Secondary batteries	6
Table 3: Taxonomy of Supercapacitors[16].....	7
Table 4: Supercapacitor Performance depends on Electrolyte properties[23]	11
Table 5: Classification of electrolytes for electrochemical supercapacitors[24]	12

LIST OF FIGURES

	Page No.
Figure 1: Sources of Clean Energy	3
Figure 2: Schematic of an Electrical Double-layer Capacitor	8
Figure 3: Schematic of Energy storage of SCs types: (a) (EDLCs) ;(b) pseudo-capacitors;(c) Hybrid capacitors[20].	9
Figure 4: Supercapacitor types are based on the mechanism of energy storage[21].	10
Figure 5: Classification of SC, along with their electrode materials[22]	10
Figure 6: Ragone plot for energy storage devices [40].	15
Figure 7: Metal-organic framework (MOF) material	18
Figure 8: Hydrothermal Method	24
Figure 9: Mechanochemical Method	26
Figure 10: Microwave Method	27
Figure 11: Synthesis of Iron-Carboxylate MOF	29
Figure 12: Synthesis of Iron-Carboxylate MOF/Graphene	30
Figure 13: Synthesis of Iron-Copper MOF/Graphene.	31
Figure 14: (a) JOEL JSM-6490LA present at SCME; (b) SEM Schematic	32
Figure 15: XRD present at SCME- NUST (b) XRD basic schematic.	34
Figure 16: GAMRY Interface 1010E Potentiostat	35
Figure 17: CV plot of (a) Ideal capacitor with perfect rectangular shape (b)EDLC material with near rectangular shape(c)Pseudo capacitor with oxidation and reduction peaks[68]	37
Figure 18: GCD curves of (a) EDLC (b)Pseudo capacitor[68]	38
Figure 19: EIS (a) Equivalent circuit diagram (b)Nyquist plot	38
Figure 20: XRD Analysis	41
Figure 21: (a,b) PFG2, (c,d) PFG5, (e,f) PFG10, (g,h) PFG20	42
Figure 22: SEM images of (a, b) Fe-MOF, (c, d) Fe-MOF/G, and (e, f) FeCu-MOF/G. [72]	43
Figure 23: FTIR Analysis	44

Figure 24: Raman Analysis	45
Figure 25 (a-c): Schematic diagram for electrode fabrication and 3-electrode setup[78].	46
Figure 26: Specific Capacitance of Fe-MOF(a); Fe-MOF/G(b); FeCu-MOF/G(c)	48
Figure 27: GCD Curves of Fe-MOF(a); Fe-MOF/G(b); FeCu-MOF/G(c)	49
Figure 28: Specific Capacitance at different current densities of Fe-MOF; Fe-MOF/G; FeCu-MOF/G	50
Figure 29: GCD at 1 st , 3000 th and 6000 th cycle (a); Stability test (b); EIS Plot (c); Charge Transfer Resistance and Solution Resistance (d)	51

ABSTRACT

Metal-organic frameworks (MOFs) have been reported as promising electrode materials for high performance supercapacitors. Significant research has been conducted to prepare MOF composites using conductive additives such as graphene nanosheets. Furthermore, conductive redox-active metals such as Copper and Cobalt have also been incorporated into MOF structures to boost up the electrochemical performance. However, in this work we used graphene nanosheets to influence the crystallization and growth of iron-MOFs followed by the washing away of graphene. This in-situ synthesis protocol was carried out via a facile hydrothermal approach. Later, the conductive Copper was also added into the MOF to investigate its influence on the performance of electrode material. The synthesized materials (i.e., Fe-MOF, Fe-MOF/G, and FeCu-MOF/G) were tested against their electrochemical performance using a tri-electrode electrochemical system in 1M KOH solution. These MOF samples were characterized using X-ray diffraction (XRD), Scanning electron microscopy (SEM), Fourier transform infrared (FTIR) and Raman spectroscopy. The electrochemical properties of the prepared samples were analysed using cyclic voltammetry (CV), galvanostatic charge and discharge (GCD), and electrochemical impedance spectroscopy (EIS). The in-situ growth of iron-MOFs using graphene resulted in enhanced specific capacitance and higher charge/discharge stability which validates the superiority of this in-situ synthesis approach.

One of the developed electrode materials, FeCu-MOF/G, displayed a high specific capacitance of 1132 Fg^{-1} at current density of 3 A g^{-1} . Moreover, FeCu-MOF/G also showed a cyclic charge/ discharge stability of 85% for 6000 cycles at 10 A g^{-1} . The exceptional performance displayed by the developed MOFs in the presence of graphene are highlighted their potential as appropriate electrode materials for supercapacitors.

The in-situ growth of iron-MOFs using graphene resulted in enhanced specific capacitance and higher charge/discharge stability which validates the superiority of this in-situ synthesis approach.

CHAPTER 1: INTRODUCTION

Energy is defined as the ability to do work. It is the basic requirement for life. Modern civilization is only possible because people have learned how to change energy from one form to another and then use it to do work.

1.1 Increasing Demand for Energy

The energy demand is growing at a rapid rate. From charging our gadgets to traveling, every person consumes an enormous amount of energy every day and this amount is increasing with time. Except for humans, every organism's total energy demand is its supply of energy in the form of food derived directly or indirectly from the sun's energy. For humans the energy requirements are not just for heating, cooling, transport, and manufacture of goods but also those related to agriculture. Global energy demand is continuously increasing every year due to population growth and economic development. Global energy consumption significantly increased by 69.22% due to an increasing world population of 47 % from 1990 to 2020[2].

1.2 Pollution

There is growing concern that continued expansion of the world economy will cause irreparable damage to the earth's environment and a reduced quality of life for future generations[3].

Historically, fossil fuel energy has served the world for many decades beginning from the 1700s. Since the 1700s, fossil fuel energy has powered industrial production, automobiles, and the activities of corporations which have contributed to GDP growth in several countries. In the late 2000s, evidence began to emerge that fossil fuel energy contributed to the increase in greenhouse gas emissions and climate change and could negatively affect human life and animal life in the future[4].

The main change in the atmospheric composition is primarily due to the combustion of fossil fuels, used for the generation of energy and transportation. Variant air pollutants have been reported, differing in their chemical composition, reaction properties, emission,

persistence in the environment, ability to be transported in long or short distances, and their eventual impacts on human and/or animal health[5].

1.3 Climate Change and Renewable Energy

Climate change is defined as the significant variation of average weather conditions becoming, for example, warmer, wetter, or drier—over several decades or longer. It refers to long-term changes in weather conditions and temperature. Climate change is a natural process but since the 19th century, human activities have been the main contributor to climate change.

Energy production and consumption have undeniable environmental repercussions. The environmental damage linked to the production, transformation, transport, and use of different energy sources has been substantial in the past and is still far from negligible[6].

The world is fast becoming a global village due to the increasing daily requirement of energy by all populations across the world while the earth in its form cannot change. The need for energy and its related services to satisfy human social and economic development, welfare, and health is increasing. Returning to renewables to help mitigate climate change is an excellent approach that needs to be sustainable to meet the energy demand of future generations[7].

Climate change impacts are expected throughout the energy system. On the demand side, the balance of heating and cooling demand patterns is changing due to rising temperatures. On the supply side, impacts include changes to the averages and variability of wind, solar, and hydropower resources; the availability of crops for bioenergy feedstocks; costs and availability of fossil fuels due to melting sea ice and permafrost; the efficiency of PV panels, thermo-electric power plants, and transmission lines due to rising temperatures; technology downtime due to changes in the frequency and intensity of extreme weather events[8].

Fossil fuel alternatives are the key to a future with clean energy. They seem to be the only solution to meet the rising energy demands while keeping our environment intact and livable for us and our future generations. The world is moving towards renewable energy

at a fast pace to tackle climate change but not fast enough and we face the consequences in the form of floods, extremely hot summers, extremely cold winters, and others. The need of the hour is to further reduce the use of fossil fuels as an energy source and increase our pace further in adapting renewable energy sources to meet our ever-increasing energy demands.

The sources of renewable energy include solar, wind, hydro, geothermal, biomass, and tidal. These sources are replenished at a higher rate than they are consumed. These sources are plentiful and can be found abundantly all around us.

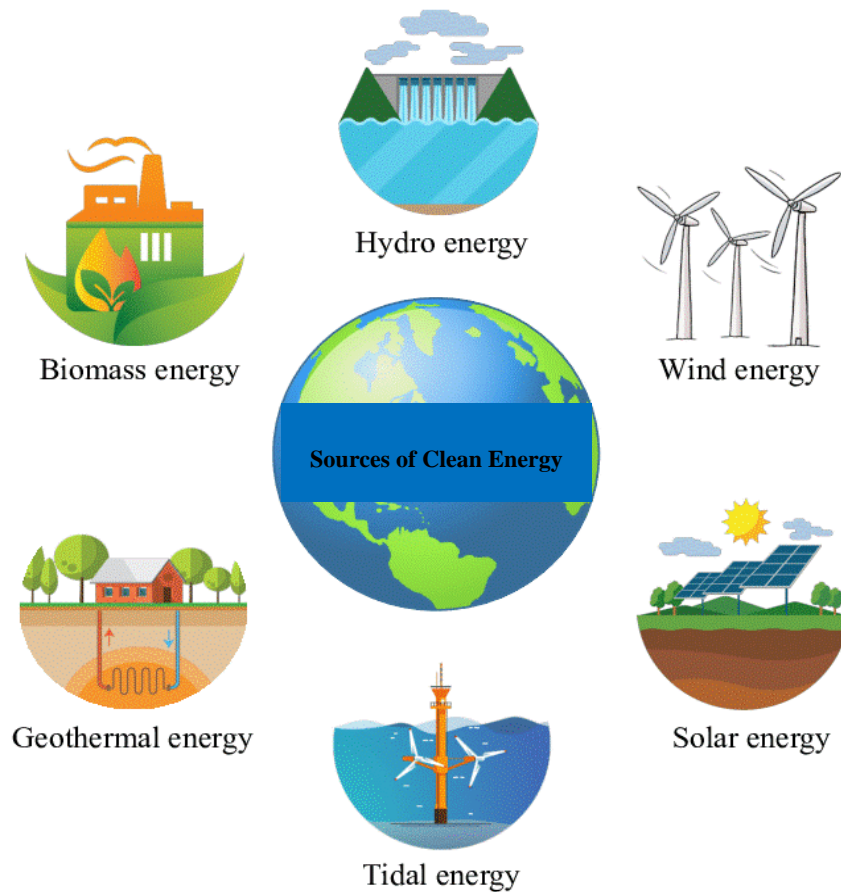


Figure 1: Sources of Clean Energy

Harnessing natural resources like wind and solar might seem the solution to all our problems, but they come with their drawbacks. Sources of renewable energy are intermittent. For example, in the case of solar energy, energy can only be generated when

the sun shines. This intermittency poses challenges to grid stability. To effectively utilize the sources of clean energy, the need for energy storage devices arises so that excess energy can be stored during peak production which can later be used during low energy generation periods.

Renewable energy has emerged as a vital solution to the pressing global challenges of climate change and energy security[9].

1.4 Energy storage devices

Energy storage devices are used to store excess energy produced and use it when energy generation is low or when demand increases. They help us in reducing imbalances in energy demand and energy production.

Energy storage systems are divided into five major categories[10]:

- Mechanical system
- Chemical system
- Electrochemical system
- Electrical system
- Thermal system

The most common energy storage devices that come in electrochemical and electrical systems are

- Batteries
- Supercapacitors

Table 1: Energy Storage Devices

Function	Supercapacitor	Lithium-ion (general)
Charge time	1–10 seconds	10–60 minutes
Cycle life	1 million or 30,000h	500 and higher
Cell voltage	2.3 to 2.75V	3.6 to 3.7V
Specific energy (Wh/kg)	5 (typical)	100–200
Specific power (W/kg)	Up to 10,000	1,000 to 3,000
Cost per Wh	\$20 (typical)	\$0.50-\$1.00 (large system)
Service life (in vehicle)	10 to 15 years	5 to 10 years
Charge temperature	–40 to 65°C (–40 to 149°F)	0 to 45°C (32°to 113°F)
Discharge temperature	–40 to 65°C (–40 to 149°F)	–20 to 60°C (–4 to 140°F)

1.4.1 Batteries

Batteries are energy storage devices that store energy and then discharge it by converting chemical energy into electrical energy. Batteries usually have one or more electrochemical cells. Batteries can be found all around us. Cellphones, laptops, and other devices around us that we use remotely while attaching a plug in a socket work on batteries.

1.4.1.1 Types of Batteries

Electrochemical batteries are classified into the following broad categories:

- Primary batteries
- Secondary batteries

Primary Batteries

Primary batteries are referred to as non-rechargeable batteries. They are discarded after they are discharged.

Secondary Batteries

Secondary batteries are referred to as chargeable batteries. They can be charged and discharged multiple times. They store energy through reversible electrochemical reactions.

Secondary batteries include[12]:

- Lead-Acid

- Nickel-Cadmium
- Nickel Metal-Hydride
- Lithium-ion

Table 2 summarizes the pros and cons of Primary and Secondary batteries[13]:

Table 2: The pros and cons of Primary and Secondary batteries

<i>Primary</i>	<i>Secondary</i>
<i>Lower initial cost.</i>	Higher initial cost.
Higher life-cycle cost (\$/kWh).	<i>Lower life-cycle cost (\$/kWh) if charging in convenient and inexpensive.</i>
<i>Disposable.</i>	Regular maintenance required.
<i>Disposable.</i>	Periodic recharging required.
<i>Replacement readily available.</i>	Replacements while available, are not produced in the same sheer numbers as primary batteries. May need to be pre-ordered.
<i>Typically lighter and smaller; thus traditionally more suited for portable applications.</i>	Traditionally less suited for portable applications, although recent advances in Lithium battery technology have lead to the development of smaller/lighter secondary batteries.
<i>Longer service per charge and good charge retention.</i>	Relative to primary battery systems, traditional secondary batteries (particularly aqueous secondary batteries) exhibit inferior charge retention.
Not ideally suited for heavy load/ <i>high discharge rate</i> performance.	<i>Superior high discharge rate performance at heavy loads</i>
Not ideally suited for load-leveling, emergency backup, <i>hybrid battery</i> , and high cost military applications.	<i>Ideally suited for load-leveling, emergency backup, hybrid battery and high cost military applications</i>
Traditionally limited to specific applications.	<i>The overall inherent versatility of secondary battery systems allows its use and continuing research for a large spectrum of applications.</i>

1.4.2 Supercapacitors

Supercapacitors are another type of electrochemical energy storage device with huge power density and specific capacitance. Supercapacitors (SCs) are energy storage devices that bridge the gap between batteries and conventional capacitors. They can store more energy than capacitors and supply it at higher power outputs than batteries. These features, combined with high cyclability and long-term stability, make SCs attractive devices for energy storage.[14].

Although batteries can accomplish transient energy storage and propulsion, the power requirements are increasing remarkably and exceed their pulse power capability. A promising way is to use a reasonable alternative solution such as Ecs[15].

Supercapacitors are being used as they can store more energy and have a prolonged life cycle. The specific capacitance is calculated as follows:

$$Q = CV$$

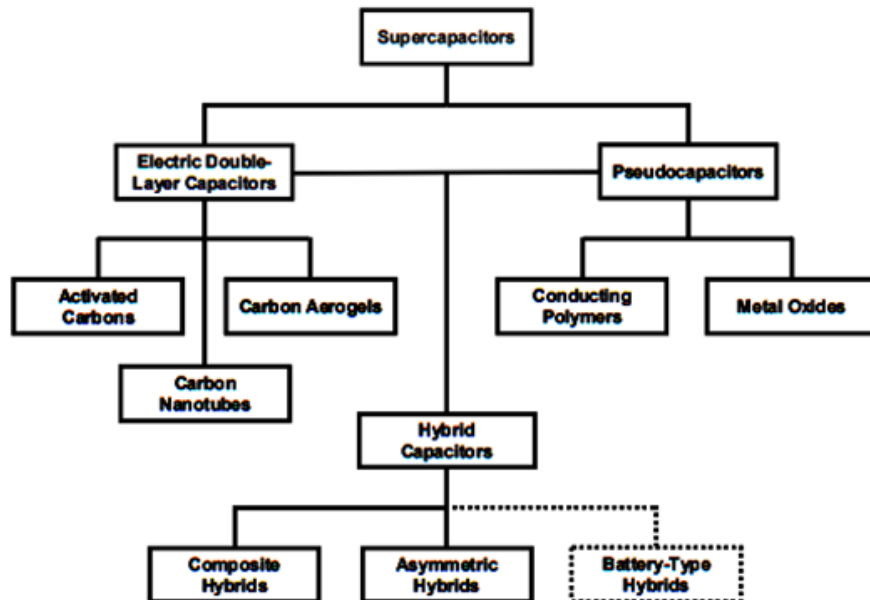
Where, C stands for specific capacitance, ' V ' for operating window, and ' Q ' for stored charge.

Because of its high-power output and low cost, SCs are a good choice for energy storage. They are divided into two groups based on the materials' compositions.

1.4.1.2 Types of Supercapacitors

Supercapacitors are classified into the following broad categories:

Table 3: Taxonomy of Supercapacitors[16]



1.4.1.2.1 Electric Double-layer Capacitors

Electrochemical double-layer capacitors (EDLCs) are constructed from two carbon-based electrodes, an electrolyte, and a separator. Like conventional capacitors, EDLCs store charge electrostatically, or non-Faradaically, and there is no transfer of charge between

electrode and electrolyte. The charge storage mechanism in EDLC is purely physical and non-faradaic, with no oxidation-reduction reaction, i.e., no active 7-electrode material. Because of the physical charge transfer, EDLC has a long cycle life.

The capacitance of an EDLC can be written as

$$C = \frac{A\epsilon}{4\pi d}$$

Where A denotes electrodes Surface area ϵ denotes dielectric constant D denotes the effective thickness of the double layer

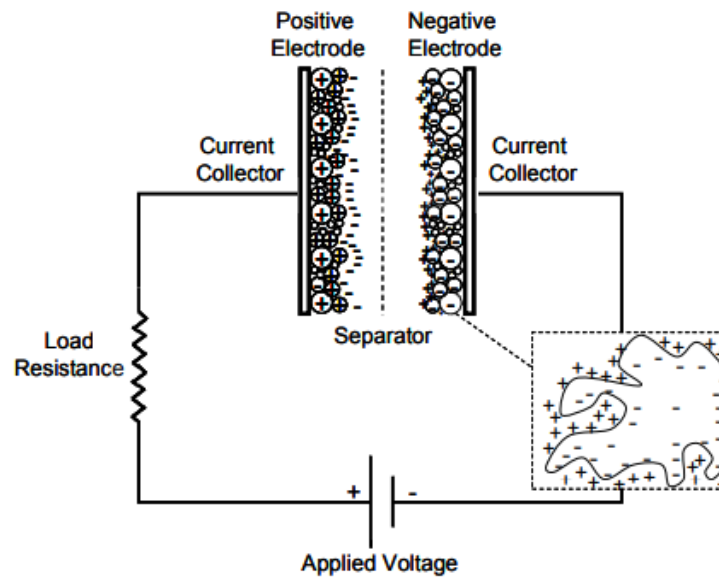


Figure 2: Schematic of an Electrical Double-layer Capacitor

Pseudo capacitors

Unlike EDLC, the pseudocapacitive reactions are faradic in origin and store electrical energy through fast and reversible redox processes at the electrode surface. In other words, pseudocapacitive materials exhibit battery-like redox reactions that happen at very high rates similar to a capacitor[17] The charge storage mechanisms in pseudocapacitive materials can involve either:

- at or near surface-redox reactions
- intercalation-type reactions

These Faradaic processes may allow pseudo capacitors to achieve greater capacitances and energy densities than EDLCs[18].

Hybrid Supercapacitors

Hybrid capacitors attempt to exploit the relative advantages and mitigate the relative disadvantages of EDLCs and pseudo capacitors to realize better performance characteristics. Utilizing both Faradaic and non-Faradaic processes to store charge, hybrid capacitors have achieved energy and power densities greater than EDLCs without the sacrifices in cycling stability and affordability that have limited the success of pseudo capacitors.

Hybrid supercapacitors are classified as either symmetric or asymmetric, with the positive electrode being a pseudo-capacitor and the negative electrode being EDLC[19].

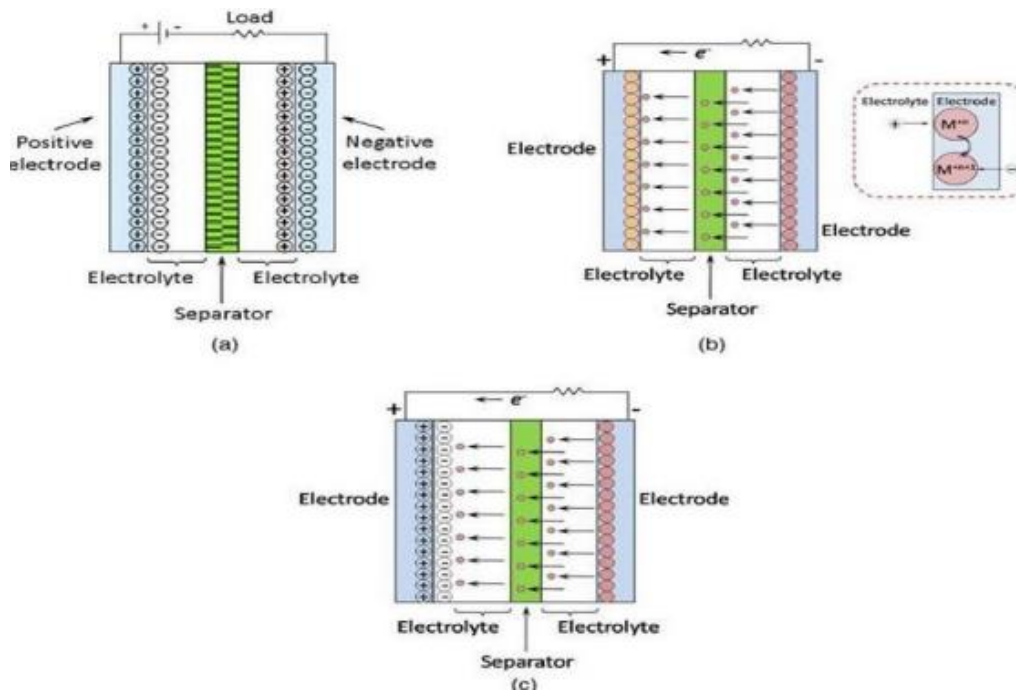


Figure 3: Schematic of Energy storage of SCs types: (a) (EDLCs) ;(b) pseudo-capacitors;(c) Hybrid capacitors[20].

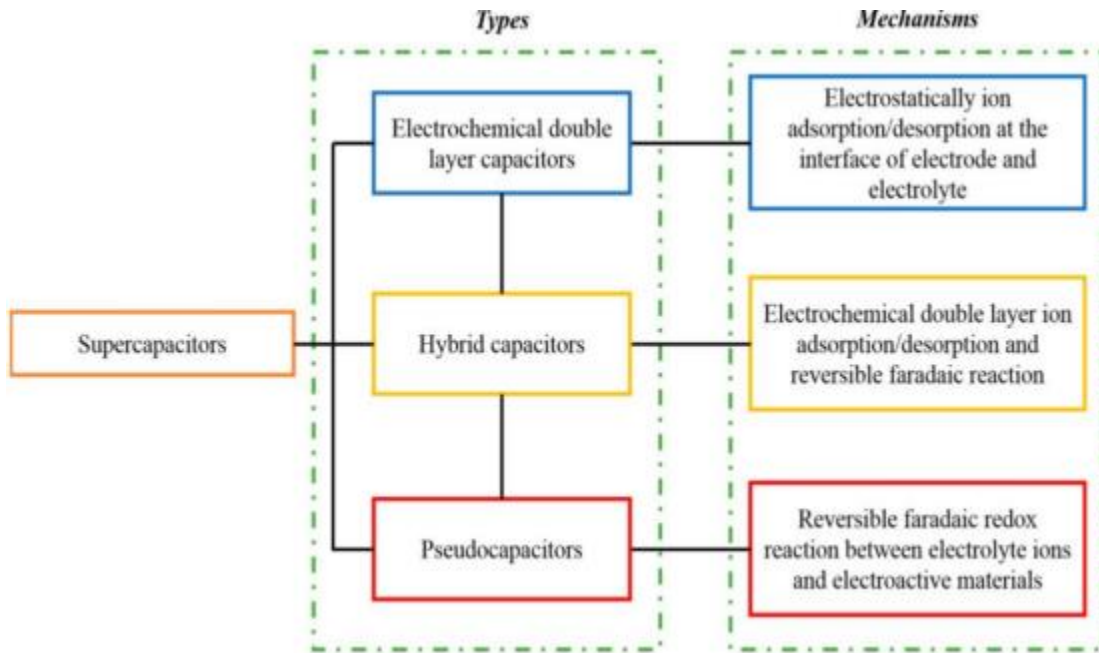


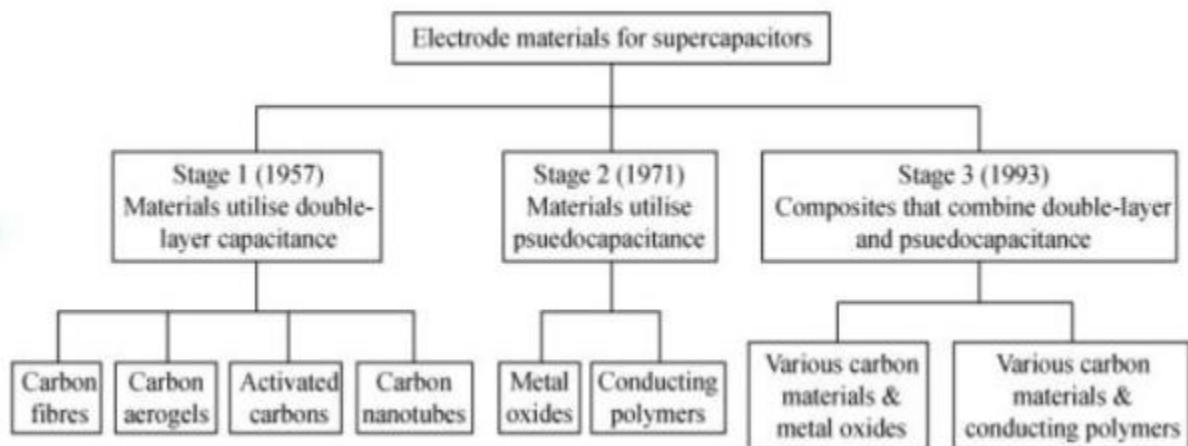
Figure 4: Supercapacitor types are based on the mechanism of energy storage[21].

2.2.6.2 Components of Supercapacitors

Electrode Materials

Electrode materials play a very important role in the performance of Supercapacitors. To obtain exceptional supercapacitor performance, the electrode materials should have high capacitance. High capacitance means more porosity and larger pore volume. The electrochemically available area might be indicated as an active electrochemical surface area.

Figure 5: Classification of SC, along with their electrode materials[22]



Electrolytes

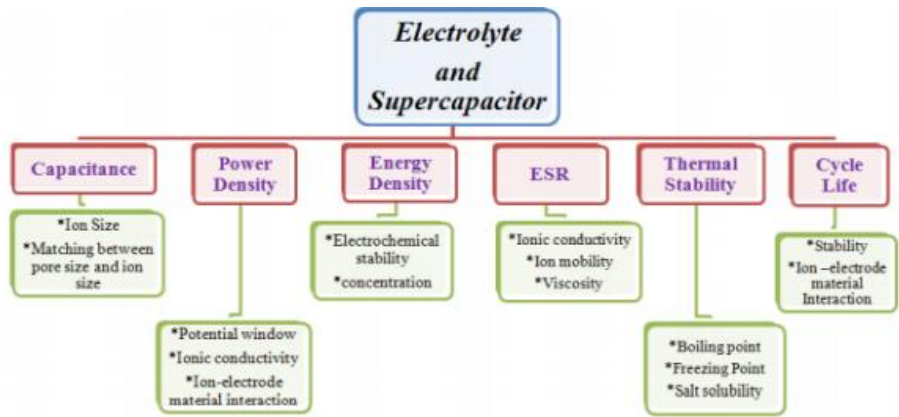
Electrolytes are utilized for the movement and conduction of ions. While fabricating a supercapacitor, our main concern is to improve its energy value which can be done in two of the following ways.

- Increasing the electrode material's capacitance
- widening the capacitor's operating potential

The ideal electrolyte material lowers internal resistance, speeds up the self-discharge process, improves power output and lifetime, and increases energy density values.

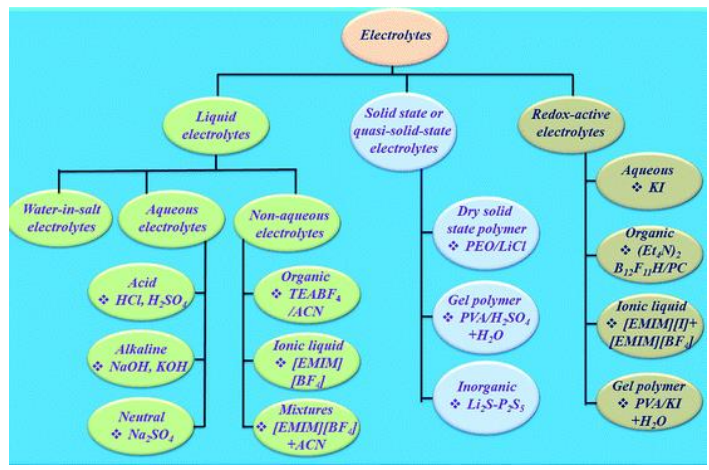
Lightweight, excellent electrical conductivity, strong electrochemical activity, and high tolerance to deterioration are all desirable qualities in an electrolyte.

Table 4: Supercapacitor Performance depends on Electrolyte properties[23]



Types of Electrolytes are listed in the following figure:

Table 5: Classification of electrolytes for electrochemical supercapacitors[24]



Liquid Electrolytes

The choice of the electrolytic material for a supercapacitor is a crucial step in the development process, which is why a lot of research has been done on various liquid electrolytic materials. Aqueous electrolytes and non-aqueous electrolytes are the two subcategories. Ionic liquids and organic electrolytes are the two further categories into which these liquid electrolytic materials are divided.

Aqueous Electrolytes

This category comprises electrolytes that consist of an aqueous solution of salts and inorganic substances. They have separated ions, which makes them extremely conductive. This makes them quite good at economically boosting power density as their lower electrolytic resistance lowers the ESR value. Another benefit of aqueous electrolytes is their ease of synthesis and handling, which qualifies them for usage in supercapacitors.

Non-Aqueous Electrolytes

Fused ions and organic salt solutions are examples of this type of electrolyte; they are more durable than aqueous electrolytes and may be applied in commercial settings. These electrolytes are also very effective to employ because they do not degrade or deteriorate even at high working potential windows. However, they do have significant drawbacks that make large-scale production difficult, such as their high cost, toxicity, and low conductivity.

Non-aqueous electrolytes

Organic Electrolytes

A conducting salt is mixed with an organic solvent to make these. They are widely commercialized as they have a broad potential window (2.5–2.8 V) which helps in increasing the energy density and improving the thermal and cyclic stability of the device.

Ionic Electrolytes:

Ionic liquids, that are composed of salts with melting points below 100 °C, are made of an asymmetric organic cation and an inorganic/organic anion. They are often consumed in their pure form or dissolved in organic solvents to evaluate their overall performance in a supercapacitor. Typically, these liquids are created by selecting various cation-anion combinations to increase the working potential window. Tetrafluoroborate is one of the anions to be selected, and the cations to be chosen are ammonium, phosphonium, pyrrolidinium, etc. (BF₄⁻).

Redox-active Electrolytes

These are further divided into two types Redox-active aqueous electrolytes These electrolytes are quite special as they can increase the overall capacitive performance of supercapacitor devices by extracting redox-based capacitance from themselves, unlike conventional supercapacitors which only rely on the redox-activity of the electrode. Some of these electrolytes include Hydroquinone, KI, lignosulfonates, etc.

Redox-active non-aqueous electrolytes

Numerous non-aqueous electrolytes have been investigated to raise the cell voltage and produce a high energy density. These electrolytes are based on organic and ionic liquids. Studies in the literature suggest that redox-active Polyfluorododecaborate cluster ions added to an organic mixture solvent including Dimethyl and Propylene Carbonate would be very helpful in increasing the pseudocapacitive contribution of carbon-based supercapacitors.

Solid and Quasi-solid (Gel) Type Electrolytes

These are extremely flexible gel electrolytes composed of a polymer matrix encapsulated in a liquid electrolyte. Because they facilitate the rapid downsizing of the electronic industries, they are attractive to work with. Liquid electrolytes are not suitable for use in portable electronic devices due to their leakage and solution resistance while having greater ionic conductivity that makes redox processes easier.

1.4.2.3 Applications of Supercapacitors

As compared to batteries, supercapacitors have an upper hand in applications where high-power density and longer life cycles over multiple charge-discharge cycles are required.

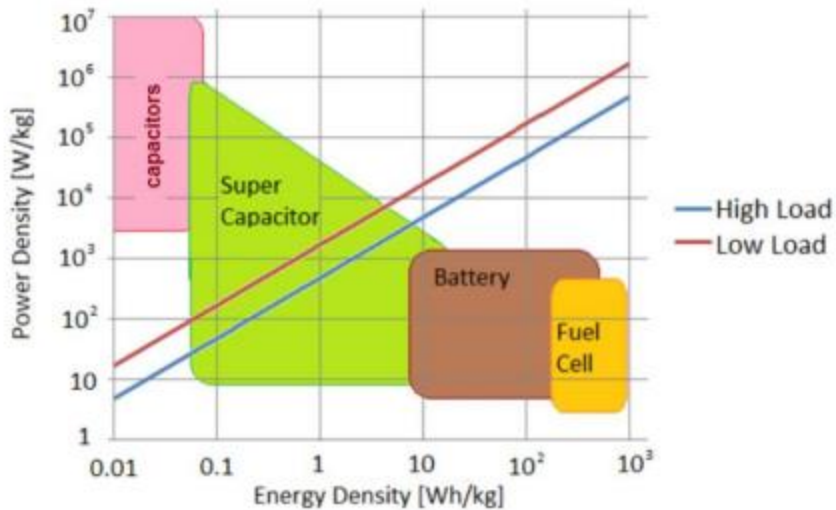


Figure 6: Ragone plot for energy storage devices [40].

Some applications of SCs are in consumer electronics [23], [24] tools, power supply [25] voltage stabilization [26] microgrid [27] renewable energy storage [28], energy harvesting [29], [30], street lights [31] medical applications [32] military and automotive applications [33], [34], [35] and energy recovery [36], [37], [38], [39].

1.5 Objectives

- Synthesis of MOFs and improving the methods of forming the iron carboxylate MOFs with desired characteristics.
- Investigating how synthesis parameters affect the structure, morphology, and size of the Iron carboxylate MOFs such as temperature, pH and the concentration of the reactants.
- Characterizing the synthesized MOFs using X-ray diffraction, scanning electron microscope, FTIR and RAMAN.
- Exploring how the electrochemical performance of iron carboxylate MOFs could be improved by the addition of conductive frameworks, for example, graphene.
- Improving electrode fabrication, such as selecting proper binder, conductive additives, and electrode's thickness.

- Performing cyclic voltammetry (CV), galvanostatic charge-discharge (GCD), and electrochemical impedance spectroscopy (EIS) on the fabricated electrodes based on the developed MOFs.
- Evaluating the specific capacitance and cycling stability of the developed electrode materials.
- Comparing the efficiency of the iron carboxylate MOF based electrodes to other superior electrode materials that have been used in designing supercapacitors.
- Suggesting research directions for future and the possible enhancements of iron carboxylate MOF-based electrodes.

CHAPTER 2: LITERATURE REVIEW

In the past two decades, electrochemical capacitors, also known as supercapacitors, have received special attention since they are one of the most promising electrochemical energy storage devices for high-power delivery or energy harvesting applications[1].

2.1 MOFs

MOFs (Metal Organic Frameworks) are porous materials made up of inorganic metal clusters also known as Secondary Building Units (SBUs) and organic linkers. This is why MOFs are often referred to as hybrid organic-inorganic materials[2]. The organic units are typically mono-, di-, tri- or tetravalent ligands[3].

2.1.1 *MOFs for next-generation energy storage devices*

With the development of society and the world becoming a global village, the need for clean energy is becoming very important globally. As modern society develops, the need for clean energy becomes increasingly important on a global scale. Because of this, the exploration of novel materials for energy storage and utilization is urgently needed to achieve a low-carbon economy and sustainable development. Among these novel materials, metal-organic frameworks (MOFs), a class of porous materials, have gained increasing attention for utilization in energy storage and conversion systems because of ultra-high surface areas, controllable structures, large pore volumes, and tunable porosities[4].

2.1.2 *Transition Metal MOFs*

Transition-metal (Fe, Co, Ni) based metal-organic framework materials with controllable structures, large surface areas, and adjustable pore sizes have attracted wide research interest for use in next-generation electrochemical energy-storage devices. Transition-metal (Fe, Co, Ni) based metal-organic frameworks and their derivatives are focused on because of their application in supercapacitors and batteries.

2.1.3 MOF Linkers

Metal-organic framework (MOF) materials use inorganic metal ions as structural centers and basic organic ligands to undergo coordination reactions under certain catalysis and temperature conditions and generate coordination bonds through coordination reactions. Molecules are connected to form a new material with porous network characteristics.

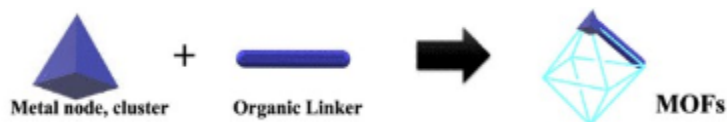


Figure 7: Metal-organic framework (MOF) material

2.1.4 MOF Uses

Their tunable porous structure is exploited by numerous different application areas such as renewable energy, environmental applications, catalysis, sensors, and biomedicine. Metal-organic frameworks (MOFs) are porous crystalline structures with high surface areas. The structure of MOFs is constituted by inorganic secondary building units (SBUs) and organic linker molecules between them.

MOFs, MOF composites, and MOF derivatives show great potential for the subject with their high porosity, hybrid structure, and tunability.

The porous structure of MOFs makes them excellent candidates for gas storage and separation.

Nanoparticle composite MOFs have various chemical and structural diversities, excessive loading capacity, and high decomposability; thus, they are beneficial to traditional nanomedicines[5]. MOFs and their composite materials have also been used as electrocatalysts for the ORR[6-8] carbon dioxide reduction[9], the HER[10], and the OER[11]. MOFs have so far attracted a lot of interest in several research fields, both with the aim of developing and synthesizing novel materials as well as for a wide range of applications. In recent years, numerous reviews of electrically conductive MOFs[12], 2D

MOFs[13], the history of activation and porosity[14], clean energy applications[15], and so on have been published.

2.1.5 *MOFs for energy storage*

MOFs, as electrode materials, offer the potential for enhancing supercapacitor performance, particularly when combined with aqueous electrolytes[16, 17].

Díaz et al. reported the initial pristine MOF used as electrode material for ELDC[18]. Lee et al. reported the first MOF as electrode material for pseudo capacitors with specific capacitance up to 206.76 F g^{-1} [19]. With different redox-active ligands and metal centers Gong, Y., Li, J., Jiang, P.G., et al. employed zinc, cadmium[20] and Campagnol, N., Romero-Vara, R., Deleu, W., et al employed iron-based MOFs[21] were employed as the electrode materials and showed pseudocapacitive performances accordingly.

Wei et al. achieved the first attempt to utilize 2D MOF as the active material for supercapacitors[22]. A Ni-based MOF with a layered structure was studied, and the specific capacitances were 1127 and 668 F g^{-1} at the current density of 0.5 and 10 A g^{-1} .

In another study[23], Wei et al. synthesized Zn-doped Ni-MOF which showed higher capacitance of 1620 and 854 F g^{-1} at the current density of 0.25 and 10 A g^{-1} , respectively. Subsequently, two-layered structures Co-MOFs synthesized by Liu, X., Shi, C., Zhai, C., et al. and Yang, J., Ma, Z., Gao, W., et al.[24, 25] displayed improved capacitances of 2474 and 2564 F g^{-1} at 1 A g^{-1} , respectively. In addition to nanosheet morphology, Yan, Y., Gu, P., Zheng, S., et al. synthesized the accordion-like Ni-MOF superstructure and examined it as pseudocapacitive material[26]. An asymmetric flexible solid-state supercapacitor established by accordion-like Ni-MOF and activated carbons was also proved to be a high-performance device. Beyond 2D MOF-based energy storage devices, Xu, J., Yang, C., Xue, Y., et al. synthesized nickel-based MOF nanorods were synthesized and exhibited pseudocapacitive behavior as well[27]. The constructed Ni-based MOF nanorods/graphene asymmetric supercapacitor achieved 166 F g^{-1} at 1 A g^{-1} . Jiao, Y., Pei, J., Chen, D., et al. and Gao, S., Sui, Y., Wei, F., et al. have proved that mixed-

metal MOFs have better electrochemical performance than the corresponding monometallic MOFs[28, 29].

Fe-MOFs have high safety due to their low cytotoxicity and high biocompatibility; thus, they have been widely used in bio-related fields, such as in drug delivery, bioimaging, and disease treatments, as well as for their antibacterial properties.

Fe-MOFs have been studied for energy storage in batteries and supercapacitors as they can optimize charge transport and charge density in metal-organic frameworks which is critical for systematic improvements in the electrical conductivity in these materials as reported by Lei Sun et al[30]. Sheta M. Sheta et al synthesized a Fe-MOF which showed excellent antimicrobial activity[31].

According to Kuaibing Wang et al. iron-series metal-based MOFs, including Fe, Co, and Ni are primarily documented as active SCs components compared with other metals due to the widespread resource of these three elements causing the cheap nature first. The second reason is that the MOF-based materials assembled from Fe, Co, and Ni metal centers usually possess abundant electrochemical redox sites[32].

In the year 2014, Fransaer et al. reported a series of Fe-MIL MOFs including MIL-100-Fe, MIL-88B-Fe, and MIL-53-Fe composited with carbon-based materials (carbon nanotubes and carbon black) to form the SCs electrodes[21].

2.1.6 Synthetic Approaches for MOFs

Many variables, including reaction duration and temperature, solvent type, organic ligand and metal ion types, node size and structural features, the crystallization kinetics, which ought to result in crystal nucleation and growth, and numerous others, influence the synthesis of MOFs.

Most of the time, ligand and metal salt solutions are mixed to create MOFs in the liquid phase. The solvent's reactivity, solubility, and redox potential are taken into consideration while selecting it. The solvent is also a significant factor in figuring out each reaction's thermodynamics and activation energy.

2.1 Graphene

Graphene, which is a single layer of carbon atoms covalently bonded in a hexagonal pattern, has attracted a lot of interest in view of its near marvelous electrical, thermal, and mechanical characteristics. Because of its high Surface Area, excellent electrical conductivity, and good mechanical properties, it is considered as a promising material to improve the electrode stuff for energy storage devices. superior properties such as electrical conductivity and mechanical integrity to the metal-organic frameworks (MOFs) derived composite materials for application in supercapacitors when graphene is incorporated. This synergy exploits the basic properties of printer to address such issues as poor conductivity and structural stability in MOFs hence improving the performance of the whole device.

Supercapacitor application of MOFs as electrode material can be enhanced in the following ways after incorporation of graphene. To begin with, charge transfer within the composite material is faster since graphene has high electrical conductivity, hence gives lower internal resistance and higher charge discharge capabilities of the supercapacitor. This leads to improved power density levels, and hence energy delivery rate in the supercapacitor. Secondly, the mechanical strength and flexibility of graphene can help hold the MOF framework together, to ensure it does not ‘crumple or deteriorate’ when cycling. This stability helps to get a longer cycle life and more uniform cycling of the electrode material. Furthermore, the MOFs and the highly developed graphene layer provide more storage surfaces so that the supercapacitor has a high capacitance and energy density.

Graphene, when present during the synthesis of MOFs, can influence the performance and properties of MOFs greatly. Although graphene has a high surface area, excellent mechanical strength, and electrical conductivity, it can also provide multiple nucleation sites during MOF synthesis which can result in many crystals with smaller crystal size. Moreover, this addition contributes to a uniform size of the MOF crystals since graphene sheets can hinder the clustering of MOF particles. Smaller and more uniformly distributed crystals can also increase the overall surface area[33, 34].

Supercapacitors and batteries are two energy storage devices where supercapacitors can store more energy than capacitors and supply it at higher power outputs than batteries. Their long-term stability and high cyclability make them attractive energy storage devices[35].

However, low capacitance[36, 37] and energy density[38, 39] adversely influences the energy storage in large amounts over a longer time period. Most of the supercapacitors usually suffer from high self-discharge rates[40, 41] which leads to the loss of stored energy when idle. The need to use multiple cells in series arises, due to the low voltage per cell [42]. Limited life cycle, as a result of material degradation, reduces the long-term stability of some electrode materials which also results in poor electrical conductivity[43]. This ultimately minimizes the charge-transport efficiency within the electrode material and at electrode/electrolyte interface. In addition, there exist serious challenges with regards to cost and environment concerning certain materials and synthesis procedures. Development of new electrode materials and advanced fabrication techniques is important to overcome these limitations in supercapacitor technology. This means that electrode materials like metal-organic frameworks (MOFs) when combined with graphene, which is a conducting material, enhance capacitance, energy density, and reduce self-discharge rate. Such materials exploit MOFs' high surface area, tunable porosity along with the excellent electrical conductivity of graphene making more efficient supercapacitor electrodes [44-46]. In order to improve performance, it is also necessary to focus on optimizing specific surface area and pore size distribution while at the same time ensuring compatibility and integration of different materials [47].

Copper-based Metal-Organic Frameworks have also emerged as promising supercapacitor electrode materials due to several intrinsic and application-oriented advantages including high electrical conductivity [48], redox activity [49], thermal and chemical stability[50] and Structural versatility[51]. Copper-based MOFs, when combined with conductive materials such as carbon nanotubes(CNTs) and graphene, leverage synergistic effects improving mechanical properties, electrical conductivity, and electrochemical stability[52] thus enhancing the overall performance.

Combining iron and copper MOFs with graphene leverages the synergistic effects of these materials enhancing the overall performance of supercapacitors. This hybrid approach offers many advantages, which include improved electrical conductivity [53], higher surface area [54], enhanced redox activity [55], and better mechanical stability [56]. All these advantages make graphene/MOF hybrids favorable materials for developing high-performance supercapacitors.

Graphene, when present during the synthesis of MOFs, can influence the performance and properties of MOFs greatly. Although graphene has a high surface area, excellent mechanical strength, and electrical conductivity, it can also provide multiple nucleation sites during MOF synthesis which can result in smaller crystal size. Moreover, this addition contributes to a uniform size of the MOF crystals since graphene sheets can hinder the clustering of MOF particles. Smaller and more uniformly distributed crystals formation as a result of graphene addition can also increase the overall surface area in MOFs [33, 34].

The present study is focused on synthesis of three porous MOF synthesized in the presence of graphene nanosheets i.e., Fe-MOF, Fe-MOF/G, and FeCu-MOF/G by a hydrothermal synthesis method and on investigating the electrochemical performance of developed samples as an electrode material for supercapacitor applications.

2.3 Methods

2.3.1 Hydrothermal/Solvothermal Method

Solvo(hydro)thermal reactions take place above the solvent's boiling point in closed vessels with autogenous pressure[57]. Most MOFs thus far have been created under solvo(hydro)thermal conditions. These reactions are typically done over lengthy periods of time (hours or even days) in closed containers (autoclaves) with polar solvents and temperatures between 50 and 260 °C. Autoclaves lined with Teflon are utilized for reactions that need temperatures higher than 400 °C. Elevating the temperature of the processes can promote bond formation, particularly when kinetically inert ions are employed, and guarantee appropriate crystallization.

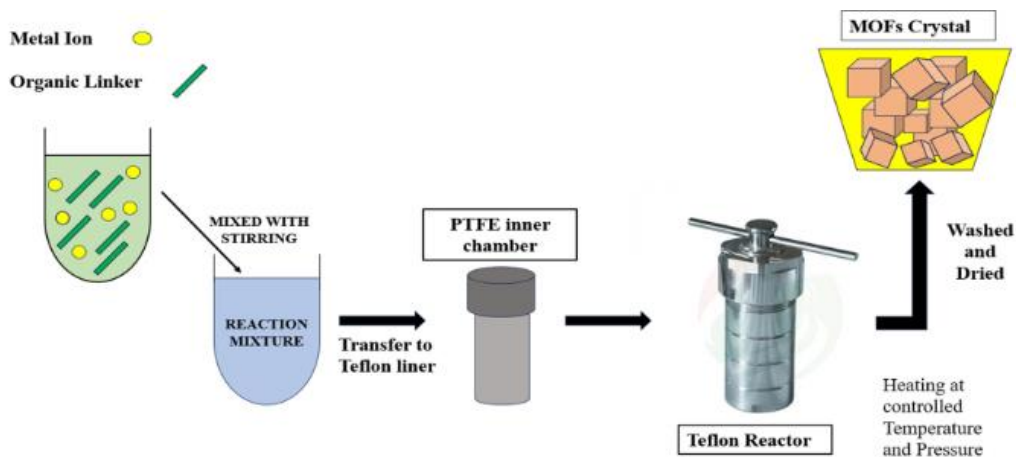


Figure 8: Hydrothermal Method

Advantages:

- Simple method
- Changing time, temperature, concentration, and solvent type allows for easy and exact morphology control.

Disadvantages:

- Expensive autoclaves and reactors
- Concerns about safety

2.3.2 *Slow Diffusion Method*

The slow diffusion method is performed at room temperature and does not need an energy supply.

The reagent solutions are layered on top of one another, divided by a layer of solvent, or progressively diffused by physical barriers that submerge them during the diffusion process. Gels are occasionally employed as diffusion and crystallization media. Following the precipitate solvent's slow diffusion into the distinct layer, crystals form at the interface between the layers[58]. In particular, the diffusion approach is applied when the products have low solubility.

2.3.3 *Electrochemical Method*

On an industrial scale, this method is used for the synthesis of MOF powders. The metal ion is provided by anodic dissolution into reaction mixtures that contain the organic ligands and electrolytes. The major advantages of this method are the slighter temperatures of reaction and quick synthesis under milder conditions, compared to the solvothermal method.

2.3.4 *Mechanochemical Method*

The method uses mechanical forces, instead of using a solvent, at room temperature, to form coordination bonds by either manual grinding of the reagents or more often in automatic ball mills. In some cases, a small amount of solvent may be added to the solid reaction mixture and succeed in obtaining one-dimensional, two-dimensional, and three-dimensional coordination polymers[59].

Advantages:

- In most cases, this procedure yields pristine-quality sheets.

Disadvantages

- This technique produces a low yield.
- Lack of scalability in this method.
- The method is only limited to small-scale production.
- Controlling sheet size and thickness is a problem.

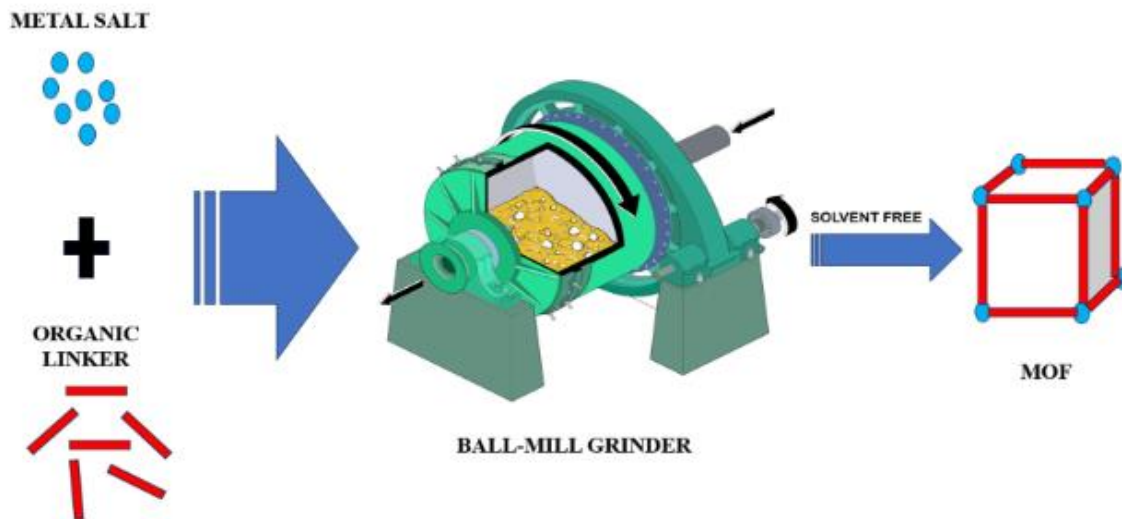


Figure 9: Mechanochemical Method

2.3.5 Microwave Method

The main factors controlling the yield and crystal development of MOFs are the energy of the microwave irradiation, the duration of exposure, the solvent concentration, and the solvent systems. Microwave irradiation has been shown to improve material characteristics and properties[60].

For many processes, the most efficient method is microwave-aided synthesis. Microwave irradiation speeds up the crystal formation of porous materials and shortens reaction times compared to traditional solvothermal synthesis, which can take days or weeks[61].

Advantages

- rapid heating, fast kinetics, phase purity, increased yield, improved dependability
- repeatability over hydrothermal synthesis

Disadvantages

- relatively high cost of equipment
- difficulty in reaction monitoring

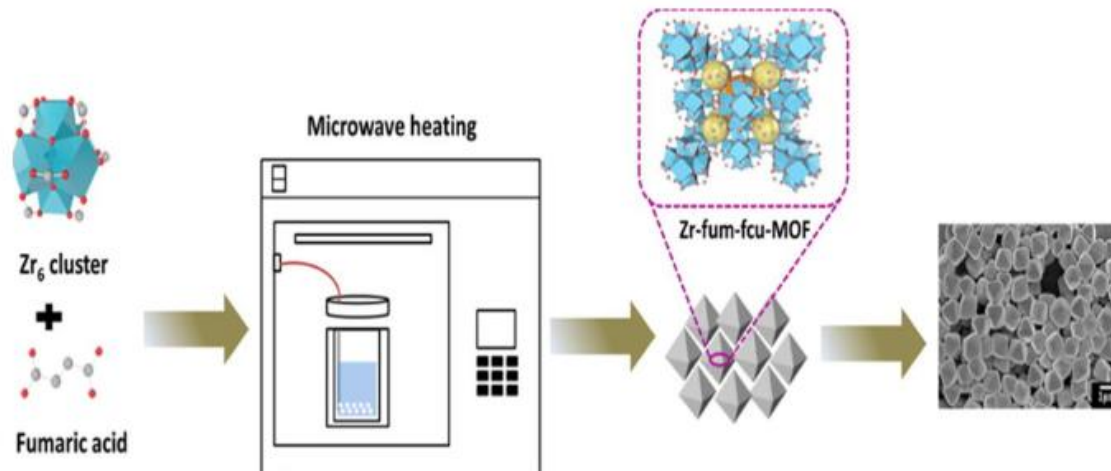


Figure 10: Microwave Method

2.3.6 Ultrasonic Method

The ultrasonication process is an inexpensive and ecologically safe way to create MOFs. It could function at room temperature and pressure and yet yield a large yield[62]. The ultrasonic-assisted synthesis offers relatively environment-friendly conditions for MOF synthesis in ambient reaction conditions (i.e., ambient temperature and atmospheric pressure) with less reaction time. Furthermore, the ultrasonic-assisted synthesis approaches avoid safety concerns, providing an opportunity to expand on the twelve principles of green chemistry[63].

Advantages:

- environment friendly
- reduced reaction time

Disadvantages:

- cannot be used for large-scale production.

CHAPTER 3: EXPERIMENTATION/SYNTHESIS

This study aims to synthesize iron-based MOFs for supercapacitor applications. This study includes:

- Synthesis of Fe-BDC MOF
- Synthesis of Fe-BDC MOF/Graphene
- Synthesis of FeCu-BDC MOF/Graphene
- Employing the synthesized MOFs as an electrode in supercapacitors
- Electrochemical performance testing of prepared MOFs
- Asymmetric supercapacitor testing by employing synthesized MOFs as positive and Activated carbon as a negative electrode material.
- Furthermore, these materials can be employed for other energy storage devices like batteries.

For this study, a Hydrothermal synthesis route has been adopted.

3.1 Materials Required

- $\text{FeCl}_3 \cdot 6\text{H}_2\text{O}$ (Iron Chloride Hexahydrate)
- H_2BDC (Terephthalic Acid)
- $\text{Cu}(\text{NO}_3)_2 \cdot 9\text{H}_2\text{O}$ (Copper nitrate Nona-hydrate)
- DMF
- Ethanol
- Graphene Powder

3.2 Apparatus Used

Apparatus used for synthesis include:

- Teflon-lined Stainless-Steel Autoclave
- Drying Oven
- Vacuum Oven

- Magnetic stirrer
- Hotplate
- Beakers
- Petri dishes
- Weighing balance
- Fume hood
- Centrifuge
- Spatula
- Pestle and Mortar

3.3 Synthesis of Iron-Carboxylate MOF

In the first step, 20ml DMF was taken in a beaker then 677mg of $\text{FeCl}_3 \cdot 6\text{H}_2\text{O}$ was added and this mixture was stirred for 2 hours. Then 206 mg of Terephthalic acid was added to this mixture and stirred for another 2 hours. This mixture was then poured into a Teflon-lined 100ml autoclave. The autoclave was placed in an oven at 120 °C for 24 hours. The precipitates were then washed multiple times alternately with DMF and ethanol several times. After washing, most of the solvent is removed in the drying oven. The obtained mud-like mixture of solvent and precipitate is then dried at 70 °C overnight. The Fe-MOF is scraped off the petri dish using a spatula and ground in a pestle and mortar to obtain Fe-MOF powder.

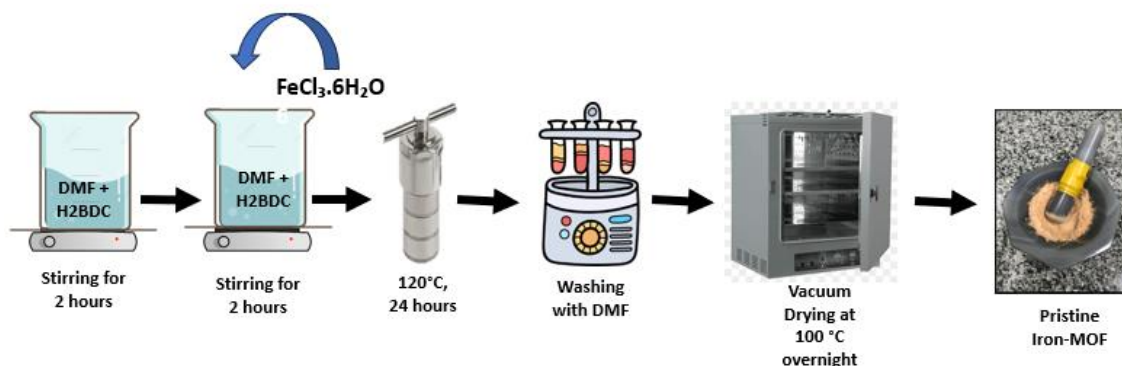


Figure 11: Synthesis of Iron-Carboxylate MOF

3.4 Synthesis of Iron-Carboxylate MOF/Graphene

In first step, 20ml DMF was taken in a beaker then 677mg of $\text{FeCl}_3 \cdot 6\text{H}_2\text{O}$ was added and this mixture was stirred for 2 hours. Then 206 mg of Terephthalic acid was added to this mixture and stirred for another 2 hours. Graphene is added according to a required percentage (2%, 5%, 10%) in 10ml DMF and sonicated for 1 hour. Both these mixtures were then combined and stirred for 1 hour. This mixture was then poured into a Teflon-lined 100ml autoclave. The autoclave was placed in an oven at 120 °C for 24 hours. The precipitates were then washed multiple times alternately with DMF and ethanol several times. After washing, most of the solvent is removed in the drying oven. The obtained mud-like mixture of solvent and precipitate is then dried at 70 °C overnight. The Fe-MOF/graphene is scraped off the petri dish using a spatula and ground in pestle and mortar to obtain Fe-MOF/graphene powder.

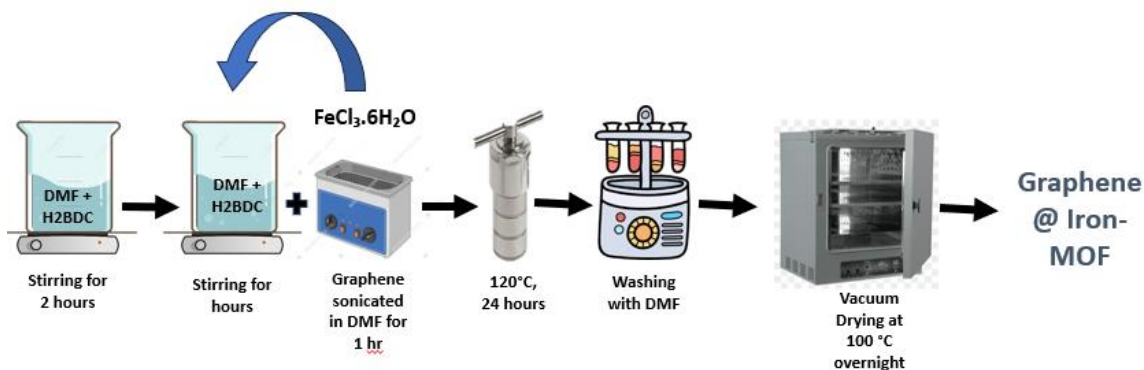


Figure 12: Synthesis of Iron-Carboxylate MOF/Graphene

3.5 Synthesis of Iron-Copper MOF/Graphene oxide

In the first step, 20ml DMF was taken in a beaker then 677mg of $\text{FeCl}_3 \cdot 6\text{H}_2\text{O}$ was added and this mixture was stirred for 2 hours. Then mg of $\text{Cu}(\text{NO}_3)_2 \cdot 9\text{H}_2\text{O}$ was added and stirred for 1 hour. Afterward, 206 mg of Terephthalic acid was in this mixture and stirred for another 2 hours. Graphene is added according to a required percentage (2%, 5%, 10%) in 10ml DMF and sonicated for 1 hour. Both these mixtures were then combined and stirred for 1 hour. This mixture was then poured into a Teflon-lined 100ml autoclave. The autoclave was placed in an oven at 120 °C for 24 hours. The precipitates were then washed

multiple times alternately with DMF and ethanol several times. After washing, most of the solvent is removed in the drying oven. The obtained mud-like mixture of solvent and precipitate is then dried at 70 °C overnight. The MOF/graphene is scraped off the petri dish using a spatula and ground in pestle and mortar to obtain MOF/graphene powder.

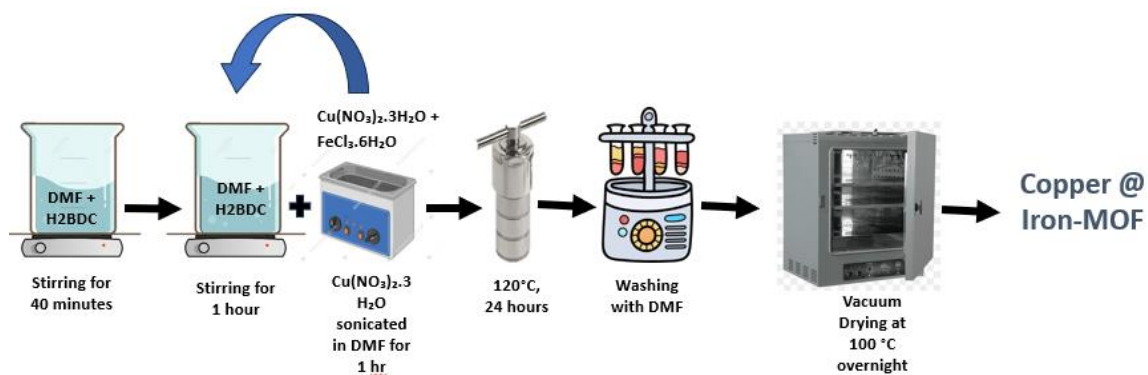


Figure 13: Synthesis of Iron-Copper MOF/Graphene.

CHAPTER 4: CHARACTERIZATION TECHNIQUES

4.1 Scanning Electron Microscopy (SEM) Analysis

This method involves focusing a fine electron beam over the surface of a specimen. It results in the removal of electrons or photons from the material's surface. These electrons are directed toward the detector. The detector's output adjusts the cathode ray tube (CRT) brightness. The material's image is created by plotting the resultant point on a CRT for every point where the beams interact[64].

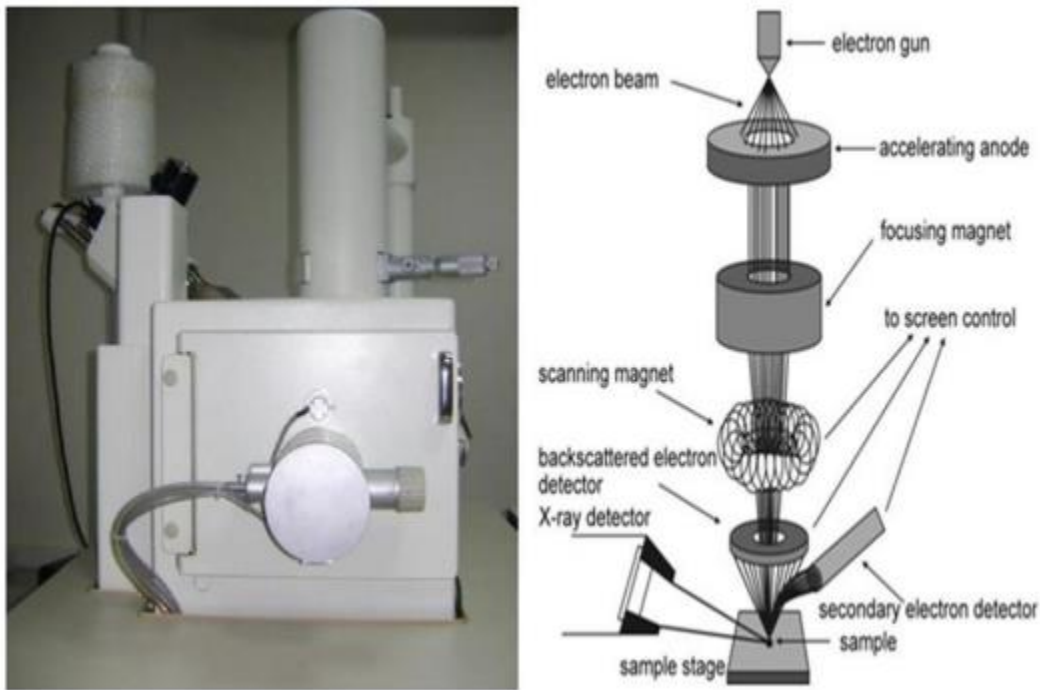


Figure 14: (a) JOEL JSM-6490LA present at SCME; (b) SEM Schematic

X-rays, backscattered electrons (BSE), and secondary electrons (SE) are released because of the electron-surface interaction. Secondary electrons are a common SEM detection method. The source of these electrons is close to the sample surface. Consequently, a distinct and clear image of the sample is produced[65]. It can disclose sample details that are even less than 1 nm. Additionally, incident electrons scatter elastically and release the scattered electrons back. Compared to secondary electrons, they emerge from deeper

regions. They thus have a somewhat poor resolution. Upon the separation of an inner shell electron from its shell, distinctive X-rays are released[66].

SEM can magnify samples from 10 to 500000 times. SEM is used to study sample morphology, chemistry, crystallography, and orientation of planes.

In this work, the morphology of the materials was examined on (JEOL-JSM- 6490LA) and FESEM analysis was performed on (MIRA3 TESCAN). Elemental composition was determined by the EDS detector attached to FESEM.

4.2 X-Ray Diffraction (XRD) Analysis

XRD is a non-destructive technique, that provides fingerprints of Bragg's reflections of crystalline materials, which determines the crystal structure of the material.

It has three primary components. a detector, sample holder, and cathode tube. Heating a filament element causes electrons to speed toward a target, where they clash with the target material to produce X-rays. Planes and layers make up a crystal. An x-ray with a wavelength comparable to these planes will therefore be reflected, resulting in an angle of incidence equal to the angle of reflection.

Diffraction that takes place is described by Bragg's law according to the following equation:

$$2d\sin\theta = n\lambda$$

When "Bragg's reflections" are detected by the detector, constructive interference is present, and Bragg's law is satisfied. Ray diffraction provides information about phase, crystallinity, and sample purity, while these reflection positions provide information about inter-layer spacing. Unit cell size, dislocations, and lattice misfits can all be found using this method.

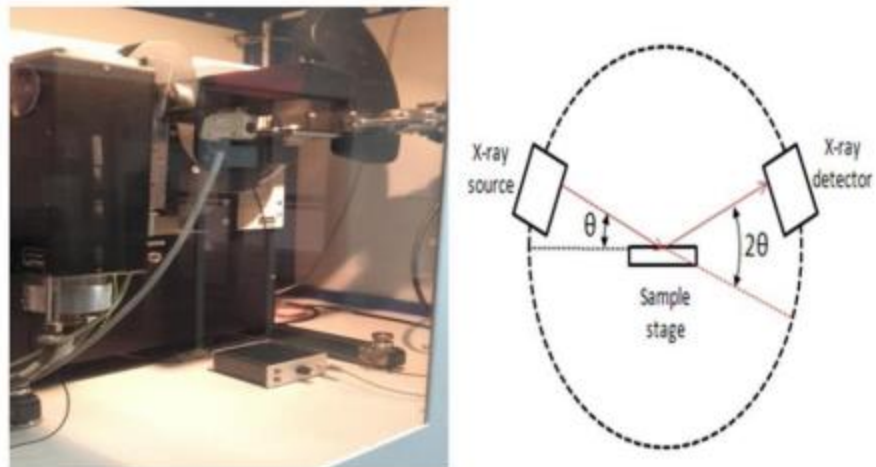


Figure 15: XRD present at SCME- NUST (b) XRD basic schematic.

4.3 RAMAN Spectroscopy

RAMAN spectroscopy is used to identify the vibrational modes of molecules, while it can also be used to examine rotational and other low-frequency modes of systems[67]. In chemistry, Raman spectroscopy is frequently utilized to provide a structural fingerprint that allows molecules to be recognized.

Raman scattering, or the inelastic scattering of photons, is the basis for Raman spectroscopy. A monochromatic light source—which can potentially include X-rays—is often derived from a laser operating in the visible, near-infrared, or near-ultraviolet ranges. The energy of the laser photons is pushed up or down because of interactions between the laser light and the system's phonons, molecules, or other excitations. The energy shift provides details on the system's vibrational modes. Usually, infrared spectroscopy provides complementary but similar information.

4.4 Fourier Transform Infrared (FTIR) Spectroscopy

Fourier-transform infrared spectroscopy (FTIR) is a technique used to obtain an infrared spectrum of absorption or emission of a solid, liquid, or gas. High-resolution spectral data over a broad spectral range are concurrently collected by an FTIR spectrometer. Compared

to a dispersive spectrometer, which measures intensity over a limited range of wavelengths at a time, this offers a substantial benefit

Fourier-transform spectroscopy is a less intuitive way to obtain the same information. Rather than shining a monochromatic beam of light (a beam composed of only a single wavelength) at the sample, this technique shines a beam containing many frequencies of light at once and measures how much of that beam is absorbed by the sample. Next, the beam is modified to contain a different combination of frequencies, giving a second data point. This process is rapidly repeated many times over a short period. Afterward, a computer takes all this data and works backward to infer what the absorption is at each wavelength.

4.5 Electrochemical Analysis

All electrochemical tests were performed on GAMRY Interface 1010E Potentiostat. This model includes everything available for running any type of electrochemical experiment.



Figure 16: GAMRY Interface 1010E Potentiostat

Following electrochemical tests were performed on this potentiostat:

- Cyclic voltammetry (CV)
- Galvanostatic Charge-Discharge (GCD)
- Electrochemical Impedance Spectroscopy (EIS)

4.5.1 CV (Cyclic Voltammetry)

It is the simplest technique on a laboratory scale to measure the electrochemical behavior. Oxidation and reduction which occur at the interface of the electrode/electrolyte can be analyzed by CV. CV system consists of a working electrode (WE), a reference electrode (RE), and a counter electrode (CE). In CV, the potential is charged on the WE and RE, and the resulting output current response is recorded between the working and counter electrodes. CV curve is plotted between the current(I) of WE vs. the potential (V). The Potential (V) is applied between the WE and the RE. Usually, Mercury/Mercury oxide (Hg/HgO) and Silver/Silver chloride (Ag/AgCl) reference electrodes were used. The counter electrode used was Platinum. The purpose of the electrolyte is to provide ions. Electrolytes must possess good conductivity. In supercapacitors, different materials show different responses. EDLC gives a rectangular curve whereas pseudo capacitor gives oxidation and reduction hump during forward and the reverse scan shows redox reactions occurring in Figure.

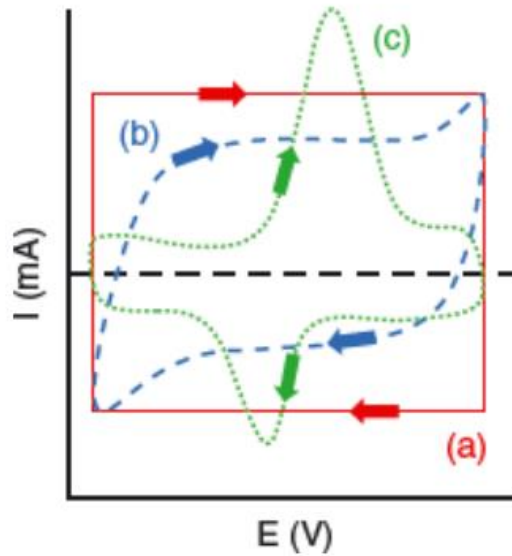


Figure 17: CV plot of (a) Ideal capacitor with perfect rectangular shape (b)EDLC material with near rectangular shape(c)Pseudo capacitor with oxidation and reduction peaks[68]

4.5.2 Galvanostatic Charge Discharge (GCD)

GCD or Galvanostatic Charge Discharge is used to study the charging and discharging of supercapacitors and batteries. In GCD we measured the change in potential with time at a constant current rate. One charge and discharge of the material is equal to one complete cycle. GCD curves of EDLC and Pseudo capacitor are different. In EDLC-type supercapacitors the charge-discharge cycles show linear curves with little IR drop whereas in the case of Pseudo capacitors the curve is not linear and the IR drop is large. This deviation refers to the charge storage mechanism that takes place due to the oxidation and reduction reactions. The linear response shows that the charge storage mechanism is not faradaic. GCD curves of both EDLC and Pseudo capacitor are in the figure.

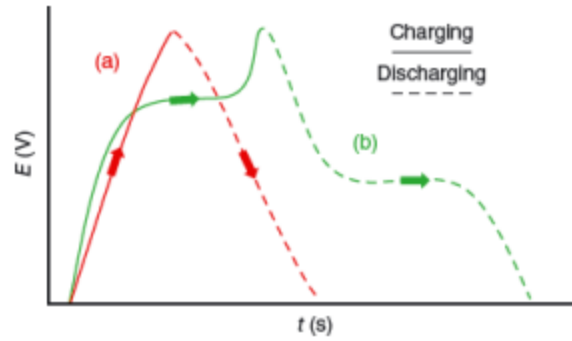


Figure 18: GCD curves of (a) EDLC (b) Pseudo capacitor [68]

Cyclic stability is an essential parameter for energy storage devices. Over multiple charge-discharge cycles, the stability of the material is studied. In labs, usually 500 to 10000 charge-discharge cycles are conducted to examine the capacitance retention of the material.

4.5.3 EIS (Electrochemical Impedance Spectroscopy)

Electrochemical Impedance Spectroscopy (EIS) is used to measure the dielectric properties of a material as a function of frequency. It measures the impedance of the material. Based on the equivalent circuit, the Nyquist plot is drawn as a response to the system. It is the impedance of a frequency.

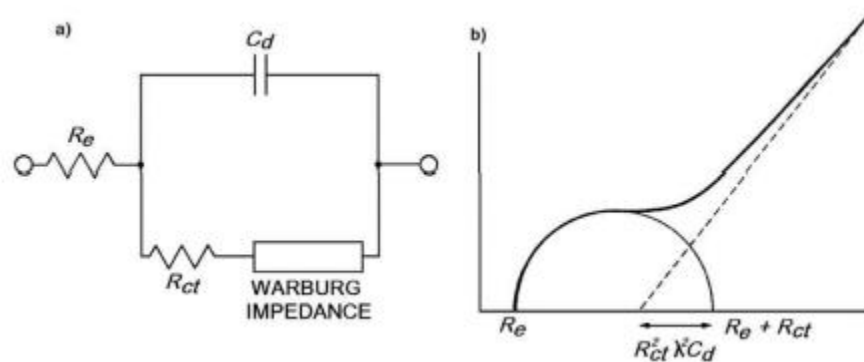


Figure 19: EIS (a) Equivalent circuit diagram (b) Nyquist plot

In the above figure, R_e is resistance which is series resistance at the working electrode-electrolyte interface, R_{ct} is charge transfer resistance or polarization resistance, and C_d is

the double layer capacitance which is interface capacitance which is between electrode and electrolyte, and Warburg impedance which depends on diffusion of reactants.

CHAPTER 5: RESULTS

5.1 XRD Results

XRD analysis was done to determine the crystal structure of the prepared materials.

XRD diffraction patterns of the synthesized Fe-MOFs are shown and compared to MIL 101 Cr (CSD number 605510 and COF number 4000663). As seen in figure 2, the Fe-MOFs have obvious absorption peaks at 2θ values of 9.35, 10.4, 12.52, 16.1, 18.76, 21.9, 26.2 and 28.4° corresponding to the (110), (101), (102), (103), (005), (202), (007), and (107) crystallographic planes respectively. The X-ray diffractogram of this Fe-MOF matches well with the one reported by Nagaraju et al [69]. The introduction of graphene increases the intensity of (101) peak in Fe-MOF/G indicating enhanced ordering or interaction with graphene. This peak disappears in FeCu-MOF/G indicating significant structural changes due to copper incorporation [70].

Upon incorporation Cu species, the sample FeCu-MOF/G displayed XRD patterns that were like that of Fe-MOFs with the exception of the broadening of (110) peak, which was attributed to the distortion of Fe-MOF structure caused by copper incorporation[71].

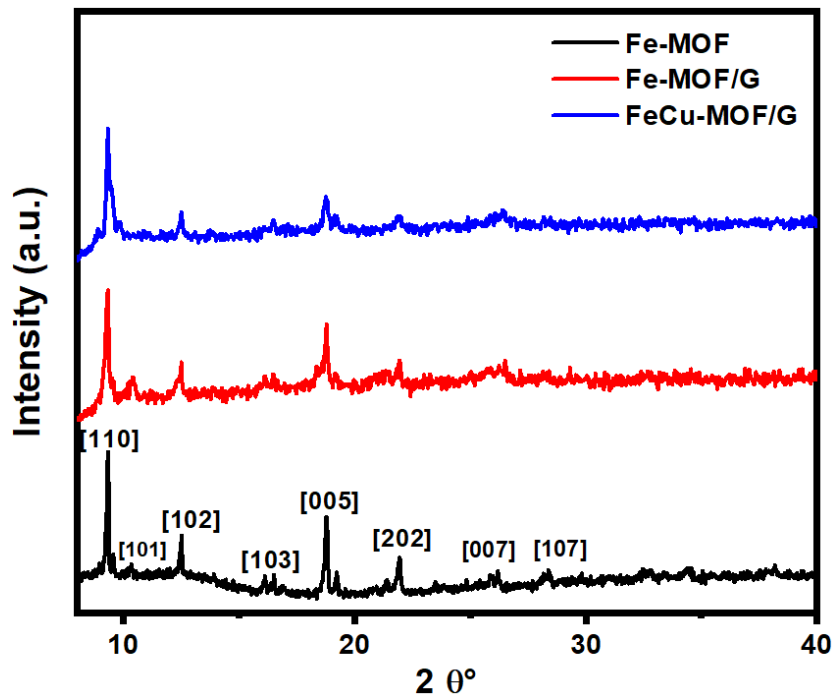


Figure 20: XRD Analysis

5.2 SEM results

To examine the morphology of the synthesized Fe-MOF, Fe-MOF/G, and FeCu-MOF/G, SEM analysis was carried out. The SEM images of Fe-MOF and Fe-MOF/G are shown and polyhedral (Octahedral) crystals are found in Fe-MOF. As the amount of Graphene increased in Fe-MOF/G, the crystal size decreased gradually. This tells us that an increase in graphene composition may limit the formation of Fe-MOF) polyhedra, and thus Fe-MOF crystals on the surface of graphene become smaller and more irregular. Four samples of each Fe-MOF/G and FeCu-MOF/G were synthesized with 2%, 5%, 10% and 20% graphene.

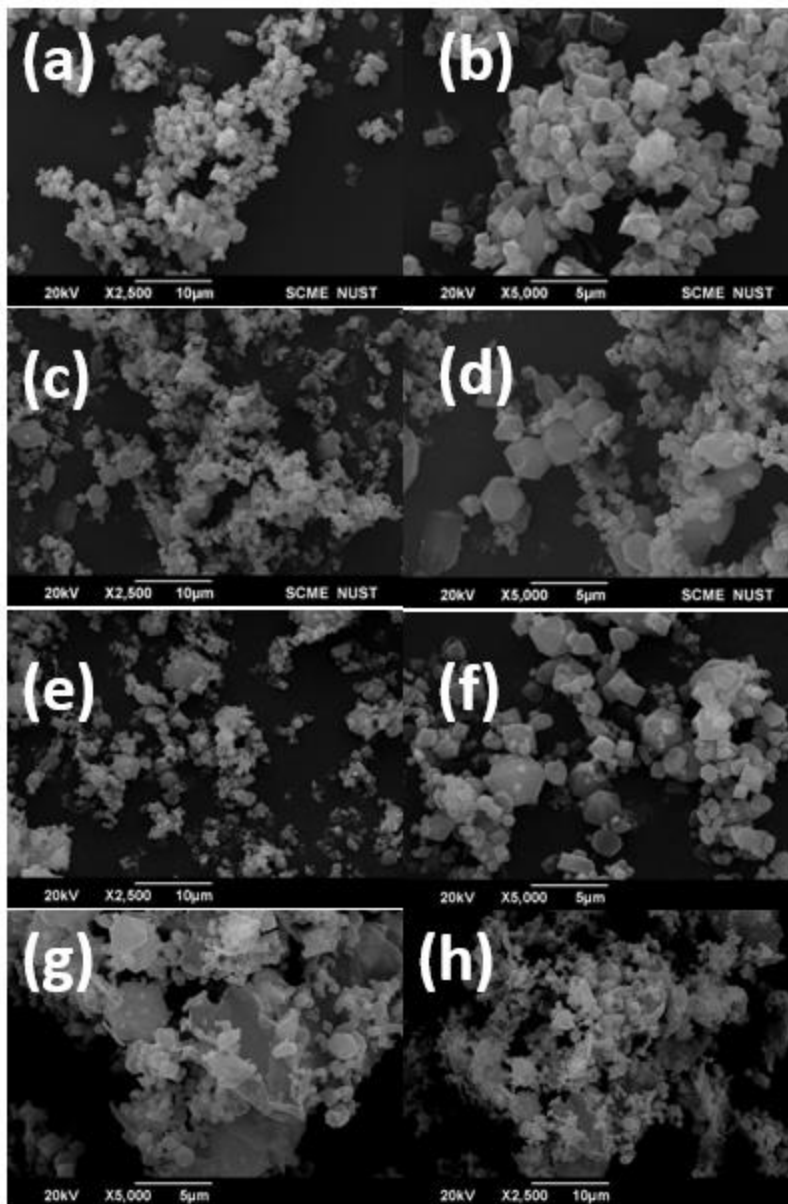


Figure 21: (a,b) PFG2, (c,d) PFG5, (e,f) PFG10, (g,h) PFG20

The samples with 10% graphene were selected for testing as they showed regular crystals.

After the selection of Fe-MOF with 10% graphene, Copper was introduced into the sample. Two samples were prepared where one sample was synthesized with 33 wt% copper nitrate and the other sample was synthesized with 67 wt% copper nitrate. The XRD and SEM analysis suggested that the sample synthesized with 33 wt% copper nitrate be used as it showed regular spherical crystals in SEM.

The FeCu/G MOF has spherical crystals and graphene sheets can be observed. A smaller amount of graphene sheets resulted in more regular crystals.

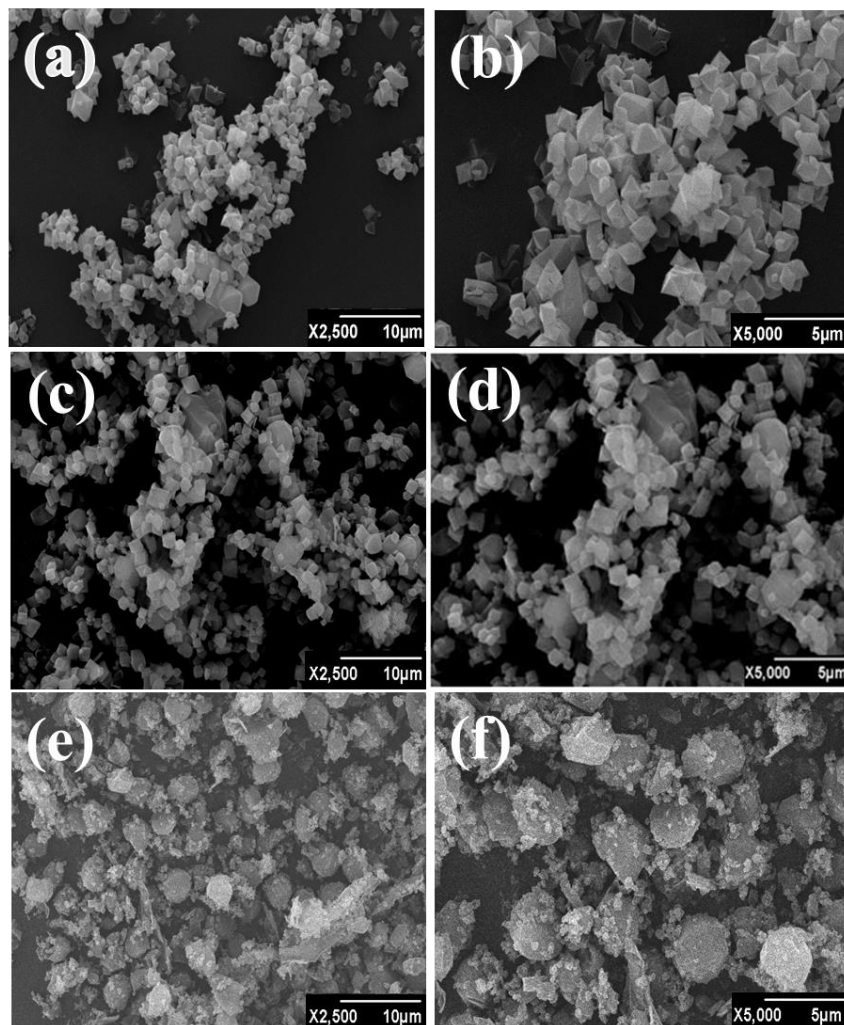


Figure 22: SEM images of (a, b) Fe-MOF, (c, d) Fe-MOF/G, and (e, f) FeCu-MOF/G. [71]

In the SEM analysis of FeCu-MOF/G, Spherical crystals are observed on graphene sheets.

5.3 FTIR Results

The characteristic peaks in Fourier Transform Infrared (FTIR) analysis located at 552, 749, 1016, 1390, and 1598 cm^{-1} proved the successful formation of Fe-MOF and is shown in

Fig. 4. Most of the Fe-MOFs characteristic peaks also appeared in the other two samples, Fe-MOF/G and FeCu-MOF/G, indicating that the structure of Fe-MOF remained stable. The peak at 552 cm^{-1} represented Fe-O bonds[72], while 749 and 1016 cm^{-1} peaks corresponded to C-H and C-O-C bending vibrations respectively. The peaks at 1390 and 1582 cm^{-1} represented the symmetric and asymmetric vibrations of O-C=O. Furthermore, the peak at 1702 cm^{-1} represented C=O vibrations in Carboxyl groups. which appeared in all three samples[73]. The peaks at 2935 and 3414 corresponded to COOH and OH groups[74, 75].

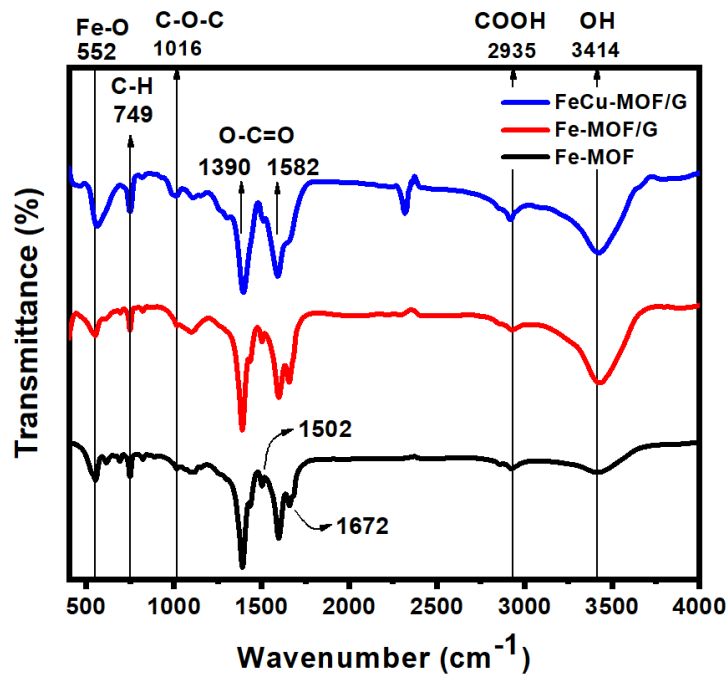


Figure 23: FTIR Analysis

Due to the interaction of graphene's -OH and -COOH functional groups with those of Fe-MOF, the peaks at 2935 cm^{-1} in both FeCu-MOF/G and Fe-MOF/G grew weaker [71]. The SEM results may explain why graphene agglomerates inhibited the formation of Fe-MOF in FeCu-MOF/G or Fe-MOF/G, as the peak of Fe-MOF in FeCu-MOF/G or Fe-MOF/G at 1502 cm^{-1} and 1390 cm^{-1} became slightly weaker [76]. The strength of the Fe-MOF/G signal at 1672 cm^{-1} altered, indicating a graphene contact. Both Fe-MOF/G and FeCu-MOF/G exhibited the typical peaks of Fe-MOF, suggesting that the MOF's crystal structure

persisted in both MOFs. New metal-oxygen interactions were suggested by additional peaks or changes in intensity in the 550-600 cm^{-1} range (Fe-O and Cu-O) [4].

5.4 Raman Results

The G and D bands of Graphene are located at 1600 and 1353 cm^{-1} . Several bands of Fe-MOF are mainly related to the organic ligands, the bands at 1433 and 1145 cm^{-1} are assigned to C=O in the carboxylic group and the C-C bond of the benzene ring, respectively, and the band appeared at 860 cm^{-1} is assigned to the vibrations of C-H and the benzene ring. The C-H vibrations of the benzene ring are associated with the band at 860 cm^{-1} . C=O peak shifts and varies in intensity, indicating the incorporation of copper, which might alter the bonding environment and cause these modifications.

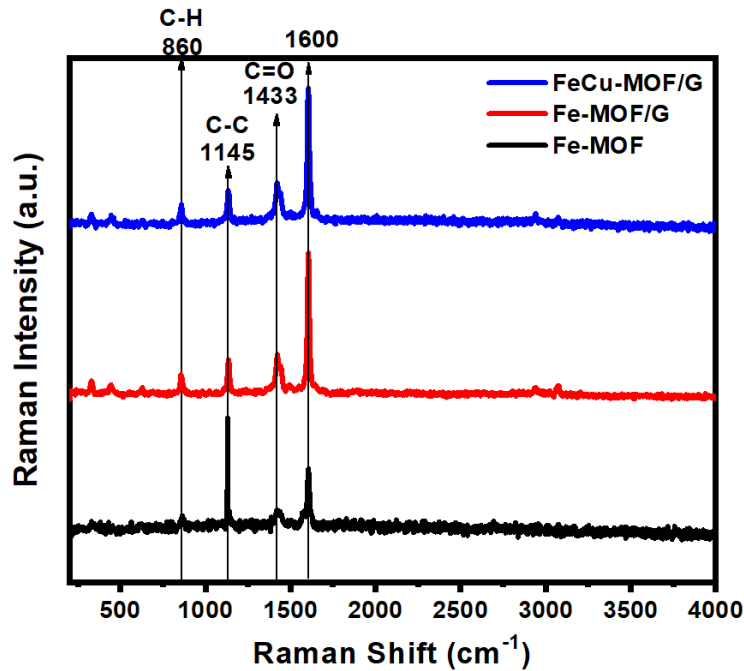


Figure 24: Raman Analysis

5.5 Electrochemical Testing

All the electrochemical tests were accompanied at room temperature using a GAMRY 1010E electrochemical workstation. The traditional slurry-coating method was used for the preparation of the working electrode. Firstly, the active material, carbon black and PVDF in the ratio of 8:1:1 was mixed in NMP and sonicated for 120 minutes to prepare slurry. Nickel foam with an area of 1cm² was pretreated, the slurry was pasted into Ni foam, and the electrode was dried under vacuum and pressed at 10 MPa. To determine the mass loading of electroactive material, the Ni foam was weighted before and after the loading of the electroactive material.

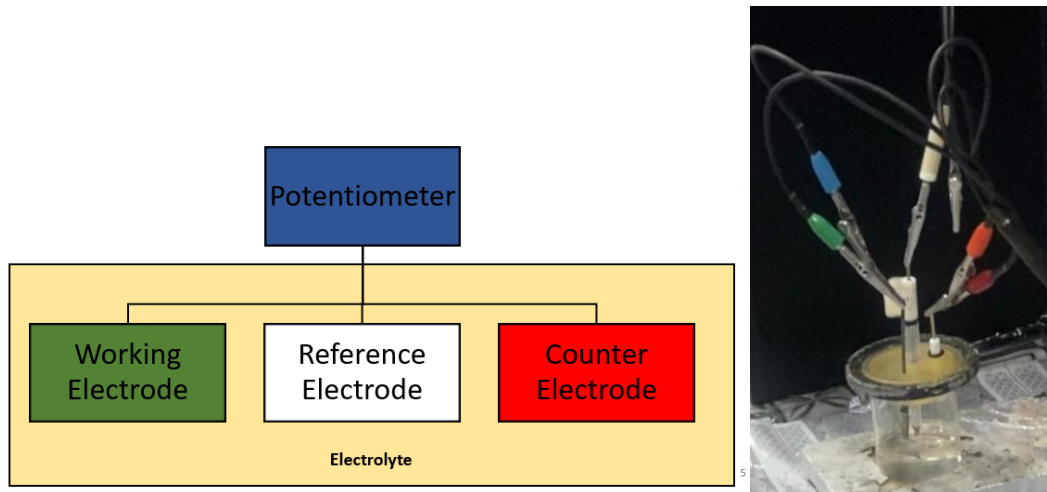


Figure 25 (a-c): Schematic diagram for electrode fabrication and 3-electrode setup[77].

To perform the electrochemical test, the electrode employed was of a relatively higher mass, in which the mass of electroactive material ranged between 3-4mg. For the analysis of the charge storage performance of the electrode, a three-electrode configuration was

employed using a 2 mol KOH solution as electrolyte. Platinum wire was used as a counter electrode while an Ag/AgCl reference electrode was employed. The CV, GCD, and EIS tests measured the charge storage performance. The specific capacitance(F/g) of an electrode was calculated from the GCD curves using the equation:

$$C_s = (I*t)/(m*\Delta V) \dots\dots\dots (1)$$

Where,

“t” is discharge time(s),

“I” represents current density(A),

“m” is mass of active material(g),

ΔV is the voltage drop during discharge(V).

5.5.1 CV (Cyclic Voltammetry)

Cyclic Voltammetry has been carried out to determine the faradaic response of the synthesized MOFs at different scan rates in the range of 5 mV s⁻¹ to 100 mVs⁻¹ with a potential window of 0 V to 0.42 V. The nonrectangular shape is shown.

confirms the faradaic redox reaction and the pseudocapacitive nature of MOF electrode materials. Redox peaks were observed in the CV curves of the MOFs. The peak positions of samples were at different ranges which represented the unconventional materials having different polarization. Increasing the scan rate, peaks shifted from their position showing that the different polarization and redox reaction is limited in less prominent peaks. With the increase in the scan rate, the specific capacitance decreases as there would be limited faradaic redox reaction as the availability of the active sites would be lesser in comparison to the lowest scan rate at which the capacitance would be high due to the availability of more redox active sites.

The specific capacitance of all three MOFs was calculated at different scan rates by using:

$$C_s = (\int i dV)/(V_s*m*\Delta V)\dots\dots\dots (6)$$

Here C_s represents specific capacitance, $\int idv$ is the integrated scan area, V_s represents scan rate, m is the active mass which was 0.004 mg and ΔV is the operating potential window.

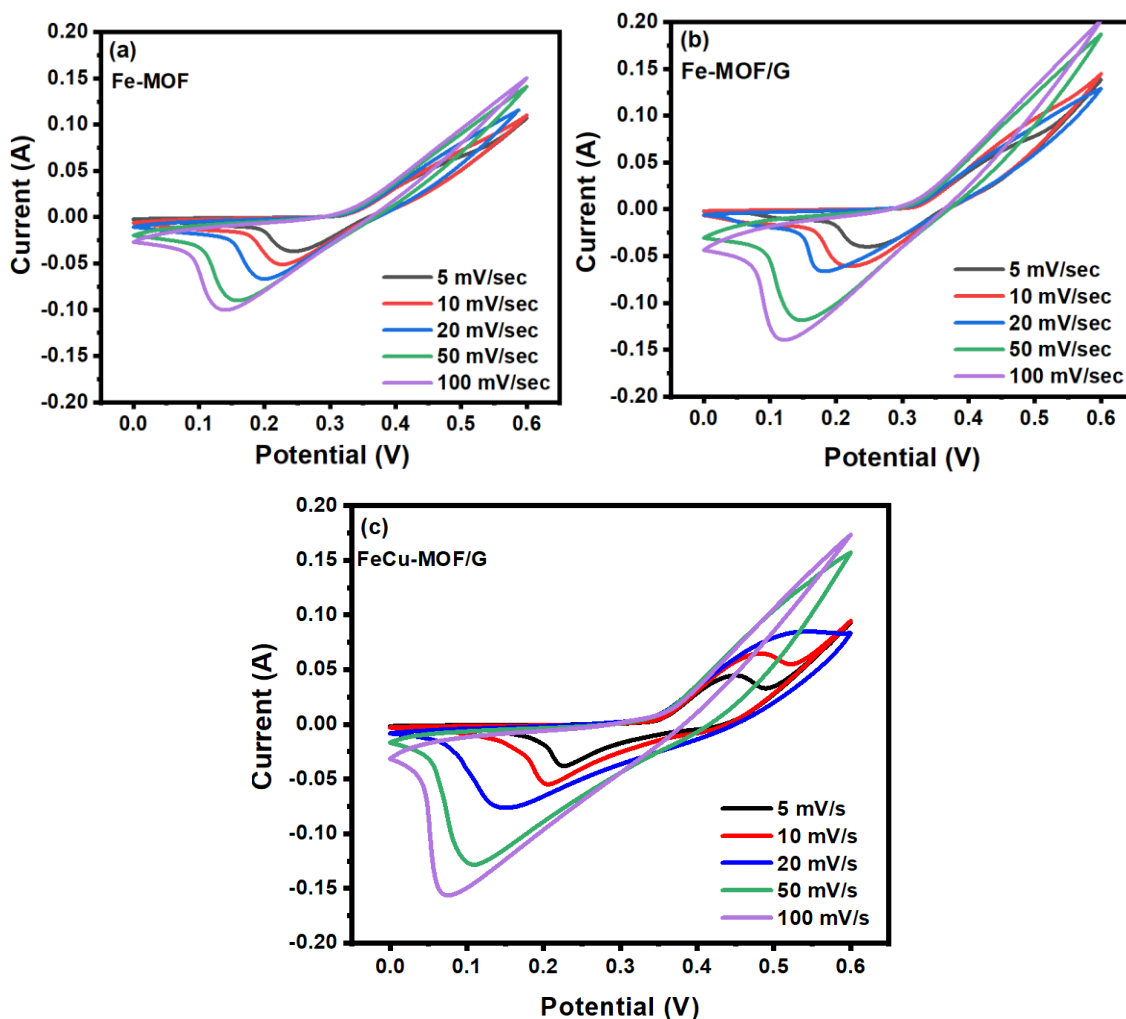


Figure 26: Specific Capacitance of Fe-MOF(a); Fe-MOF/G(b); FeCu-MOF/G(c)

5.5.2 GCD (Galvanostatic Charge/Discharge)

GCD curves of the MOFs were plotted from the range of 3 A g⁻¹ to 7 A g⁻¹ in the operating window of 0 V to 0.42 V. Faradaic behavior of the different MOF materials is revealed from the GCD curves as all the curves of materials show nonlinear response which suggests that faradaic reactions occur, and charge storage is due to oxidation and reduction. It is evident from the curves that FeCu/G exhibits a longer discharge time in comparison with other MOFs, suggesting that the electrochemical performance of FeCu/G is far superior

due to the replacement of the synergistic effect of both iron and copper. Also, FeCu/G shows more discharge time as compared to the other MOFs.

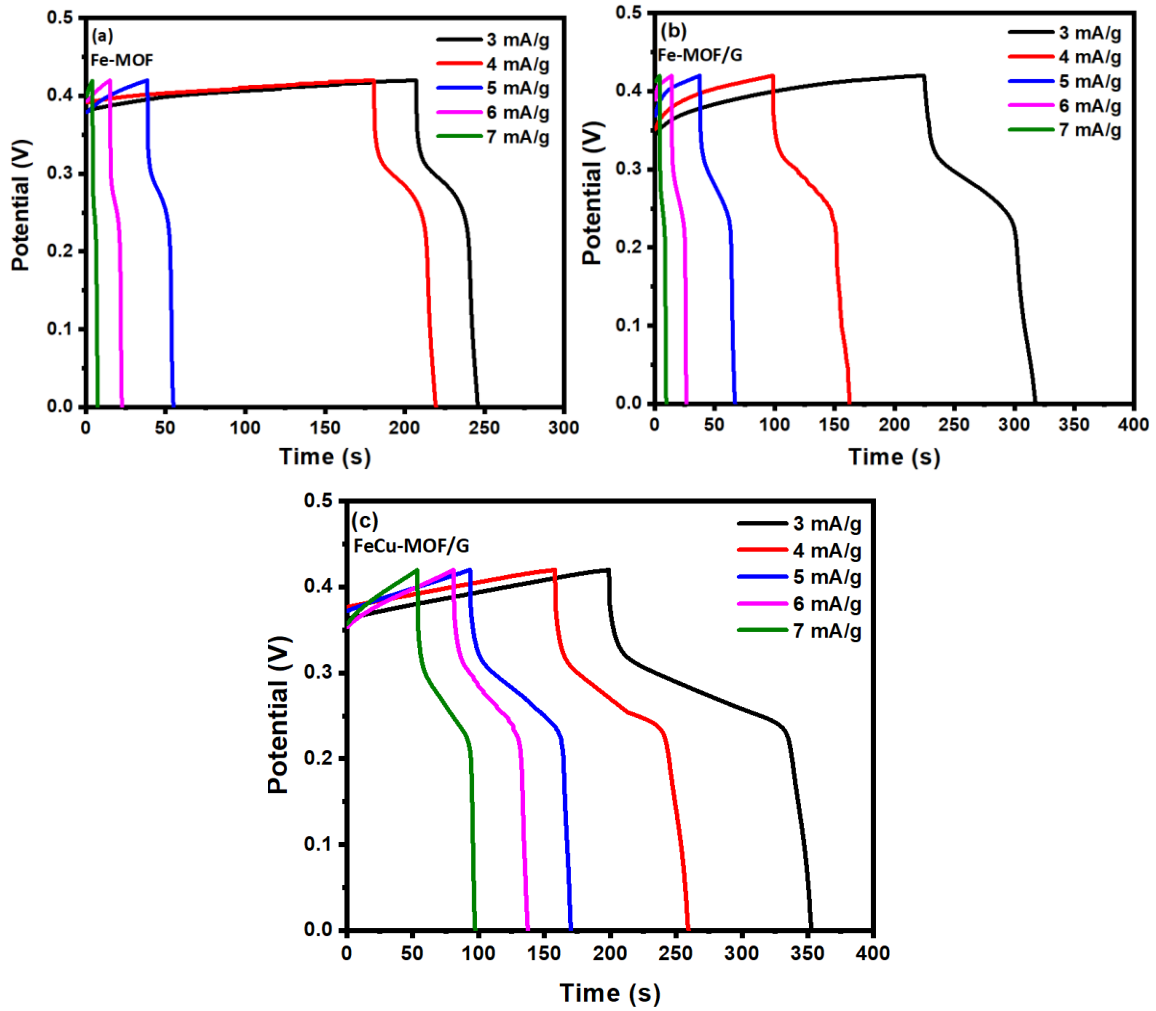


Figure 27: GCD Curves of Fe-MOF(a); Fe-MOF/G(b); FeCu-MOF/G(c)

GCD is the most accurate way to calculate specific capacitance. Specific capacitance is calculated by:

$$C_s = (I \cdot t) / (m \cdot \Delta V) \dots\dots\dots (7)$$

Here, “t” is discharge time, “I” represents current density “m” is the mass of active material, and ΔV is the voltage drop during discharge. FeCu/G shows good specific capacitance of 1132 Ag⁻¹, 952.38 Ag⁻¹, 904.76 Ag⁻¹, 828.57 Ag⁻¹ and 725 Ag⁻¹ at 3 A g⁻¹, 4 A g⁻¹,

5 A g⁻¹ , 6 A g⁻¹ and 7 A g⁻¹ as shown in Fig. Moreover, Fe-MOF and Fe-MOF/G exhibit less performance as compared to FeCu-MOF/G.

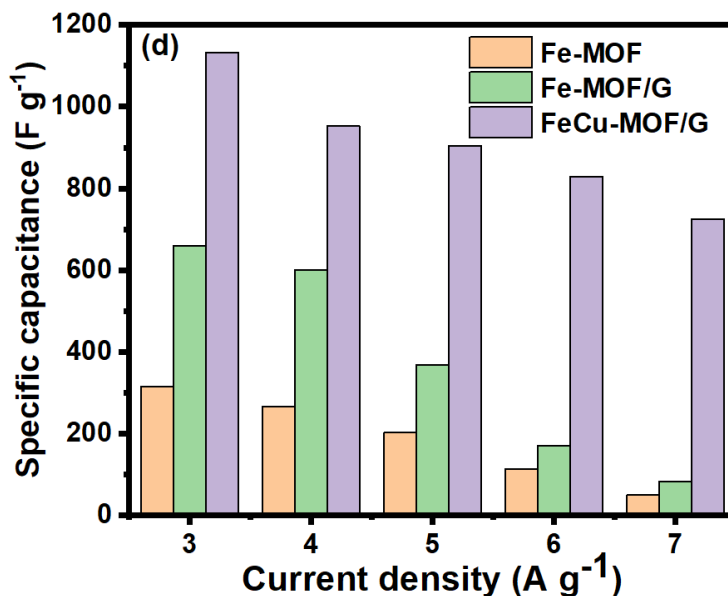


Figure 28: Specific Capacitance at different current densities of Fe-MOF; Fe-MOF/G; FeCu-MOF/G

5.5.3 EIS (Electrochemical Impedance Spectroscopy)

For the analysis of the charge transfer resistance (R_{ct}) and solution resistance (R_s), EIS was performed. The Nyquist plot consists of the R_{ct} , which is the measure of the difficulty encountered when an electron is shifted from one atom or compound to another. It is quite like other forms of electrical resistance. The higher the value of R_{ct} measurement, the greater the energy that is lost during the charge transfer. FeCu/G shows the lowest R_{ct} value which means that electrons must face less resistance which results in excellent electrochemical performance of the material. The minimum R_s and R_{ct} values of all the samples affirmed that all three samples are excellent supercapacitor materials but as FeCu/G has the minimum R_{ct} value, it is the best material for supercapacitor among all three samples. The Nyquist plot in Table shows the R_{ct} values of all samples.

5.5.4 Cyclic Stability

The cyclic stability rate performance of the FeCu/G was tested by running 6000 cycles at 10Ag-1. It exhibited excellent cyclic performance with 85% capacity retention throughout the cycles. The extraordinary performance of FeCu/G is due to the introduction of graphene and bimetallic' s synergistic effect. They aid in improving conductivity and electrochemical active sites, resulting in high rate-capability and capacitance.

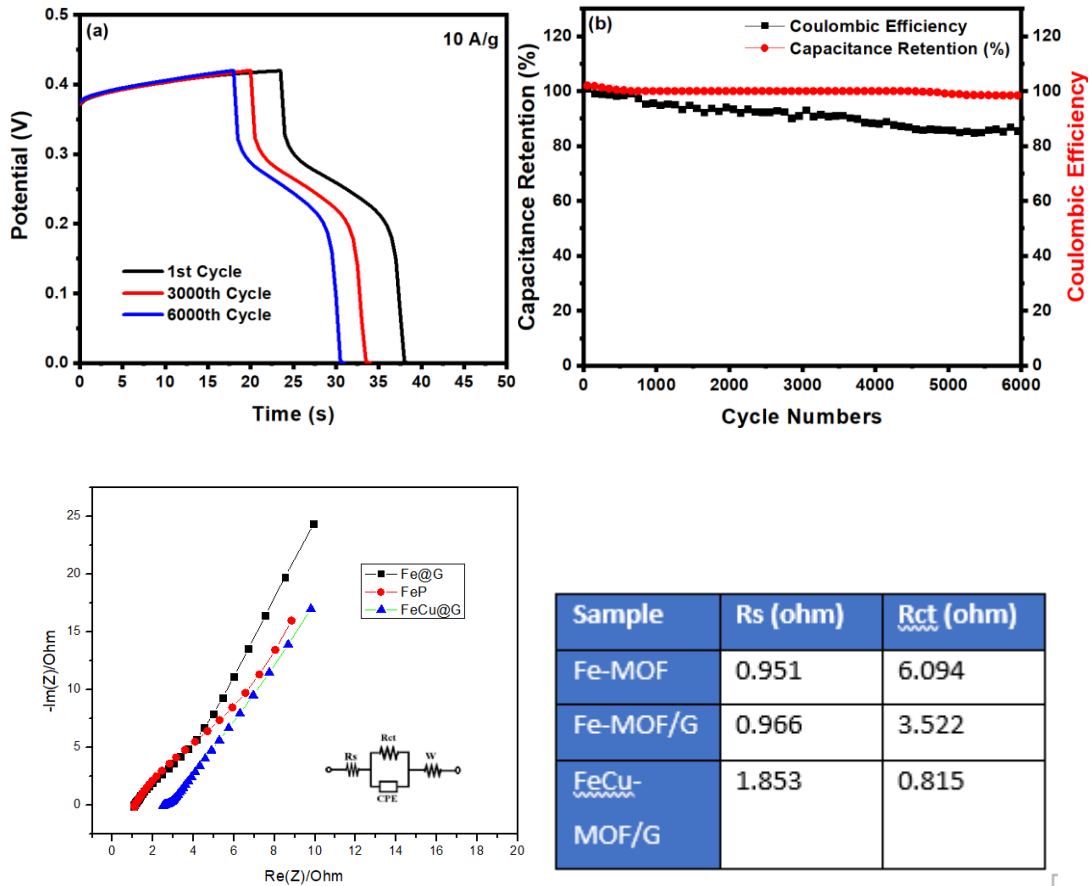


Figure 29: GCD at 1st, 3000th and 6000th cycle (a); Stability test (b); EIS Plot (c); Charge Transfer Resistance and Solution Resistance (d)

CHAPTER 6: CONCLUSION

This comprehensive study sheds light on the significant advancements in supercapacitor electrode materials. Synthesis, characterization, and electrochemical performance evaluation of Fe-MOF, Fe-MOG/G and FeCu-MOF/G composites have provided valuable insights into their potential for practical applications as electrode material for supercapacitors. Developed composites displayed excellent electrochemical properties. FeCu-MOF/G exhibited highest specific capacitance value of 1132 F g^{-1} at a current density of 3 A g^{-1} . FeCu-MOF/G electrode also demonstrated high cyclic stability and displayed capacitance retention of 85 % after 6000 cycles at 10 A g^{-1} current density. The outstanding electrochemical properties of developed composites was attributed to the presence graphene providing ample nucleation sites resulting in smaller MOFs crystallite size resulting in high surface area as well as bimetallic's synergistic effect of Fe and Cu present in the sample. This synergy provides the higher surface adsorption sites when coupled with the high electrical conductivity of Cu, enhances the ionic diffusion and improved electrochemical interactions resulting in lower ESR values.

Furthermore, the findings of this research pave the way for future investigations, such as exploring different synthetic approaches to optimize the composite material's properties, investigating its long-term stability under cycling conditions, and scale-up production for commercial use. It is evident that the MOF and graphene composites hold tremendous promise for addressing the ever-growing demand of high-performance energy storage materials in the renewable energy sector.

Future Outlook

The findings of this research pave the way for future investigations, such as exploring different synthetic approaches to optimize the MOF material's properties, investigating its long-term stability under cycling conditions, and scale-up production for commercial use. It is evident that the MOF synthesized in the presence of graphene hold tremendous promise for addressing the growing demand for high-performance energy storage materials in the renewable energy sector.

As the quest for sustainable and efficient energy storage solutions continues, it is imperative to leverage the knowledge gained from this study and collaborate across interdisciplinary fields to drive innovation in supercapacitor technology. With further exploration and development, the Fe-MOF and graphene have the potential to revolutionize the landscape of energy storage, contributing to the advancement of green energy solutions and addressing global environmental challenges.

REFERENCES

1. Simon, P. and Y. Gogotsi, *Materials for electrochemical capacitors*. Nature materials, 2008. **7**(11): p. 845-854.
2. Batten, S.R., et al., *Terminology of metal–organic frameworks and coordination polymers (IUPAC Recommendations 2013)*. Pure and Applied Chemistry, 2013. **85**(8): p. 1715-1724.
3. Czaja, A.U., N. Trukhan, and U. Müller, *Industrial applications of metal–organic frameworks*. Chemical Society Reviews, 2009. **38**(5): p. 1284-1293.
4. Zhang, X., et al., *Metal–organic frameworks (MOFs) and MOF-derived materials for energy storage and conversion*. Electrochemical Energy Reviews, 2019. **2**: p. 29-104.
5. Sharmin, E. and F. Zafar, *Introductory chapter: metal organic frameworks (MOFs)*, in *Metal-organic frameworks*. 2016, IntechOpen.
6. Yasin, G., et al., *Tailoring of electrocatalyst interactions at interfacial level to benchmark the oxygen reduction reaction*. Coordination Chemistry Reviews, 2022. **469**: p. 214669.
7. Kumar, A., et al., *Molecular-MN₄ vs atomically dispersed M–N₄–C electrocatalysts for oxygen reduction reaction*. Coordination Chemistry Reviews, 2021. **446**: p. 214122.
8. Kumar, A., et al., *A catalyst-free preparation of conjugated poly iron-phthalocyanine and its superior oxygen reduction reaction activity*. Chemical Engineering Journal, 2022. **445**: p. 136784.
9. Yang, Y., et al., *Efficient nanomaterials for harvesting clean fuels from electrochemical and photoelectrochemical CO₂ reduction*. Sustainable Energy & Fuels, 2018. **2**(3): p. 510-537.
10. Nadeem, M., et al., *Pt-M bimetallic nanoparticles (M= Ni, Cu, Er) supported on metal organic framework-derived N-doped nanostructured carbon for hydrogen evolution and oxygen evolution reaction*. Journal of Power Sources, 2018. **402**: p. 34-42.
11. Yasin, G., et al., *Defects-engineered tailoring of tri-doped interlinked metal-free bifunctional catalyst with lower gibbs free energy of OER/HER intermediates for overall water splitting*. Materials Today Chemistry, 2022. **23**: p. 100634.

12. Xie, L.S., G. Skorupskii, and M. Dinca, *Electrically conductive metal–organic frameworks*. *Chemical reviews*, 2020. **120**(16): p. 8536-8580.
13. Chakraborty, G., et al., *Two-dimensional metal-organic framework materials: synthesis, structures, properties and applications*. *Chemical Reviews*, 2021. **121**(7): p. 3751-3891.
14. Zhang, X., et al., *A historical overview of the activation and porosity of metal–organic frameworks*. *Chemical Society Reviews*, 2020. **49**(20): p. 7406-7427.
15. Li, X., et al., *Metal–organic frameworks as a platform for clean energy applications*. *EnergyChem*, 2020. **2**(2): p. 100027.
16. Nagaraju, G., et al., *High-performance hybrid supercapacitors based on MOF-derived hollow ternary chalcogenides*. *Energy Storage Materials*, 2021. **35**: p. 750-760.
17. Ramulu, B., et al., *Design of high-mass loading metal–organic framework-based electrode materials with excellent redox activity for long-lasting electrochemical energy storage applications*. *Chemical Engineering Journal*, 2023. **455**: p. 140905.
18. Díaz, R., et al., *Co₈-MOF-5 as electrode for supercapacitors*. *Materials letters*, 2012. **68**: p. 126-128.
19. Lee, D.Y., et al., *Unusual energy storage and charge retention in Co-based metal–organic-frameworks*. *Microporous and Mesoporous Materials*, 2012. **153**: p. 163-165.
20. Gong, Y., et al., *Novel metal (II) coordination polymers based on N, N'-bis-(4-pyridyl) phthalamide as supercapacitor electrode materials in an aqueous electrolyte*. *Dalton Transactions*, 2013. **42**(5): p. 1603-1611.
21. Campagnol, N., et al., *A hybrid supercapacitor based on porous carbon and the metal-organic framework MIL-100 (Fe)*. *ChemElectroChem*, 2014. **1**(7): p. 1182-1188.
22. Xiao, Y., et al., *Facile surface properties engineering of high-quality graphene: toward advanced Ni-MOF heterostructures for high-performance supercapacitor electrode*. *ACS Applied Energy Materials*, 2019. **2**(3): p. 2169-2177.
23. Yang, J., et al., *Zn-doped Ni-MOF material with a high supercapacitive performance*. *Journal of Materials Chemistry A*, 2014. **2**(44): p. 19005-19010.
24. Liu, X., et al., *Cobalt-based layered metal–organic framework as an ultrahigh capacity supercapacitor electrode material*. *ACS applied materials & interfaces*, 2016. **8**(7): p. 4585-4591.

25. Yang, J., et al., *Layered structural co-based MOF with conductive network frames as a new supercapacitor electrode*. Chemistry–A European Journal, 2017. **23**(3): p. 631-636.
26. Yan, Y., et al., *Facile synthesis of an accordion-like Ni-MOF superstructure for high-performance flexible supercapacitors*. Journal of Materials Chemistry A, 2016. **4**(48): p. 19078-19085.
27. Xu, J., et al., *Facile synthesis of novel metal-organic nickel hydroxide nanorods for high performance supercapacitor*. Electrochimica Acta, 2016. **211**: p. 595-602.
28. Jiao, Y., et al., *Mixed-metallic MOF based electrode materials for high performance hybrid supercapacitors*. Journal of Materials Chemistry A, 2017. **5**(3): p. 1094-1102.
29. Gao, S., et al., *Dandelion-like nickel/cobalt metal-organic framework based electrode materials for high performance supercapacitors*. Journal of colloid and interface science, 2018. **531**: p. 83-90.
30. Sun, L., et al., *Is iron unique in promoting electrical conductivity in MOFs?* Chemical science, 2017. **8**(6): p. 4450-4457.
31. Sheta, S.M., S.R. Salem, and S.M. El-Sheikh, *A novel Iron (III)-based MOF: Synthesis, characterization, biological, and antimicrobial activity study*. Journal of Materials Research, 2022. **37**(14): p. 2356-2367.
32. Wang, K., Y. Guo, and Q. Zhang, *Metal–organic frameworks constructed from iron-series elements for supercapacitors*. Small structures, 2022. **3**(5): p. 2100115.
33. Mazlan, N.A., et al., *The growth of Metal–Organic Frameworks in the presence of graphene oxide: A Mini Review*. Membranes, 2022. **12**(5): p. 501.
34. Nazir, M.A., et al., *MOF@ graphene nanocomposites for energy and environment applications*. Composites communications, 2023: p. 101783.
35. Castro-Gutiérrez, J., A. Celzard, and V. Fierro, *Energy storage in supercapacitors: Focus on tannin-derived carbon electrodes*. Frontiers in materials, 2020. **7**: p. 217.
36. Simon, P. and Y. Gogotsi, *Materials for electrochemical capacitors nature materials*. 2008.
37. Wang, G., L. Zhang, and J. Zhang, *A review of electrode materials for electrochemical supercapacitors*. Chemical Society Reviews, 2012. **41**(2): p. 797-828.

38. Conway, B.E., *Electrochemical supercapacitors: scientific fundamentals and technological applications*. 2013: Springer Science & Business Media.
39. El-Kady, M.F. and R.B. Kaner, *Scalable fabrication of high-power graphene micro-supercapacitors for flexible and on-chip energy storage*. *Nature communications*, 2013. **4**(1): p. 1475.
40. Chmiola, J., et al., *Anomalous increase in carbon capacitance at pore sizes less than 1 nanometer*. *science*, 2006. **313**(5794): p. 1760-1763.
41. Zhang, L.L. and X. Zhao, *Carbon-based materials as supercapacitor electrodes*. *Chemical society reviews*, 2009. **38**(9): p. 2520-2531.
42. Arulepp, M., et al., *Influence of the solvent properties on the characteristics of a double layer capacitor*. *Journal of Power Sources*, 2004. **133**(2): p. 320-328.
43. Zhai, D.D., et al., *Integrating surface functionalization and redox additives to improve surface reactivity for high performance supercapacitors*. *Electrochimica Acta*, 2019. **323**: p. 134810.
44. Wang, F., et al., *Latest advances in supercapacitors: from new electrode materials to novel device designs*. *Chemical Society Reviews*, 2017. **46**(22): p. 6816-6854.
45. Mu, C., et al., *Redox and conductive underwater adhesive: an innovative electrode material for convenient construction of flexible and stretchable supercapacitors*. *Journal of Materials Chemistry A*, 2022. **10**(13): p. 7207-7217.
46. Shah, S.S. and M.A. Aziz, *Recent Advancements in Light-responsive Supercapacitors*. *Current Nanoscience*, 2024. **20**(1): p. 74-88.
47. Dojčinović, M.P., I. Stojković Simatović, and M.V. Nikolić, *Supercapacitor Electrodes: Is Nickel Foam the Right Substrate for Active Materials?* *Materials*, 2024. **17**(6): p. 1292.
48. Ding, M., et al., *Carbon capture and conversion using metal–organic frameworks and MOF-based materials*. *Chemical Society Reviews*, 2019. **48**(10): p. 2783-2828.
49. Jiang, Q., et al., *A redox-active 2D metal–organic framework for efficient lithium storage with extraordinary high capacity*. *Angewandte Chemie International Edition*, 2020. **59**(13): p. 5273-5277.
50. Ma, Z.L., et al., *A thermally and chemically stable copper (II) metal–organic framework with high performance for gas adsorption and separation*. *Inorganic Chemistry*, 2021. **60**(9): p. 6550-6558.

51. Furukawa, H., et al., *The chemistry and applications of metal-organic frameworks*. Science, 2013. **341**(6149): p. 1230444.
52. Guo, Z., et al., *Electrochemical performance of graphene and copper oxide composites synthesized from a metal-organic framework (Cu-MOF)*. RSC advances, 2013. **3**(41): p. 19051-19056.
53. Liu, C., et al., *Advanced materials for energy storage*. Advanced materials, 2010. **22**(8): p. E28-E62.
54. Hu, B., et al., *Engineering carbon materials from the hydrothermal carbonization process of biomass*. Advanced materials, 2010. **22**(7): p. 813-828.
55. Tang, J. and J. Wang, *Fe-based metal organic framework/graphene oxide composite as an efficient catalyst for Fenton-like degradation of methyl orange*. RSC advances, 2017. **7**(80): p. 50829-50837.
56. Wang, H., et al., *Ni (OH)₂ nanoplates grown on graphene as advanced electrochemical pseudocapacitor materials*. Journal of the American Chemical Society, 2010. **132**(21): p. 7472-7477.
57. Rabenau, A., *The role of hydrothermal synthesis in preparative chemistry*. Angewandte Chemie International Edition in English, 1985. **24**(12): p. 1026-1040.
58. Lazarou, K.N., et al., *Network diversity and supramolecular isomerism in copper (II)/1, 2-bis (4-pyridyl) ethane coordination polymers*. Polyhedron, 2011. **30**(6): p. 963-970.
59. Friščić, T., et al., *Real-time and in situ monitoring of mechanochemical milling reactions*. Nature chemistry, 2013. **5**(1): p. 66-73.
60. Ge, J., et al., *An effective microwave-assisted synthesis of MOF235 with excellent adsorption of acid chrome blue K*. Journal of Nanomaterials, 2019. **2019**: p. 1-8.
61. Joseph, J., et al., *Iron-based metal-organic framework: Synthesis, structure and current technologies for water reclamation with deep insight into framework integrity*. Chemosphere, 2021. **284**: p. 131171.
62. Vinoth, V., et al., *Sonochemical synthesis of silver nanoparticles anchored reduced graphene oxide nanosheets for selective and sensitive detection of glutathione*. Ultrasonics sonochemistry, 2017. **39**: p. 363-373.
63. Liu, Y., et al., *Ultrasonic-assisted synthesis, characterization, and application of a metal-organic framework: a green general chemistry laboratory project*. Journal of chemical education, 2019. **96**(10): p. 2286-2291.

64. Jerosch, J. and R. Reichelt, *Scanning electron microscopy studies of morphologic changes in chemically stabilized ultrahigh molecular weight polyethylene*. Biomedizinische Technik. Biomedical engineering, 1997. **42**(12): p. 358-362.
65. Joy, D.C. and J.B. Pawley, *High-resolution scanning electron microscopy*. Ultramicroscopy, 1992. **47**(1-3): p. 80-100.
66. Chatti, S., et al., *CIRP encyclopedia of production engineering*. 2019: Springer.
67. Graves, P. and D. Gardiner, *Practical raman spectroscopy*. Springer, 1989. **10**: p. 978-3.
68. Kim, B.K., et al., *Electrochemical supercapacitors for energy storage and conversion*. Handbook of clean energy systems, 2015: p. 1-25.
69. Nagaraju, G., et al., *Ternary MOF-based redox active sites enabled 3D-on-2D nanoarchitected battery-type electrodes for high-energy-density supercapatteries*. Nano-Micro Letters, 2021. **13**: p. 1-18.
70. Dhakshinamoorthy, A., A.M. Asiri, and H. Garcia, *Metal–organic framework (MOF) compounds: photocatalysts for redox reactions and solar fuel production*. Angewandte Chemie International Edition, 2016. **55**(18): p. 5414-5445.
71. Liu, Z., et al., *Preparation of a GO/MIL-101 (Fe) composite for the removal of methyl orange from aqueous solution*. ACS omega, 2021. **6**(7): p. 4597-4608.
72. Hamed, A., et al., *In situ synthesis of MIL-100 (Fe) at the surface of Fe₃O₄@ AC as highly efficient dye adsorbing nanocomposite*. International Journal of Molecular Sciences, 2019. **20**(22): p. 5612.
73. Ullah, S., et al., *Influence of post-synthetic graphene oxide (GO) functionalization on the selective CO₂/CH₄ adsorption behavior of MOF-200 at different temperatures; an experimental and adsorption isotherms study*. Microporous and Mesoporous Materials, 2020. **296**: p. 110002.
74. Xie, Q., et al., *Effective adsorption and removal of phosphate from aqueous solutions and eutrophic water by Fe-based MOFs of MIL-101*. Scientific reports, 2017. **7**(1): p. 3316.
75. Alshorifi, F.T., S.M. El Dafrawy, and A.I. Ahmed, *Fe/Co-MOF nanocatalysts: greener chemistry approach for the removal of toxic metals and catalytic applications*. ACS omega, 2022. **7**(27): p. 23421-23444.
76. Zheng, Y., et al., *Metal-organic frameworks/graphene-based materials: preparations and applications*. Advanced Functional Materials, 2018. **28**(47): p. 1804950.

77. Sharma, S. and P. Chand, *Supercapacitor and electrochemical techniques: A brief review*. Results in Chemistry, 2023. **5**: p. 100885.